construction engineering research laboratory

TECHNICAL REPORT C-19
June 1975

EMP SHIELDING PROPERTIES OF CONDUIT SYSTEMS AND RELATED HARDWARE

12
Cher

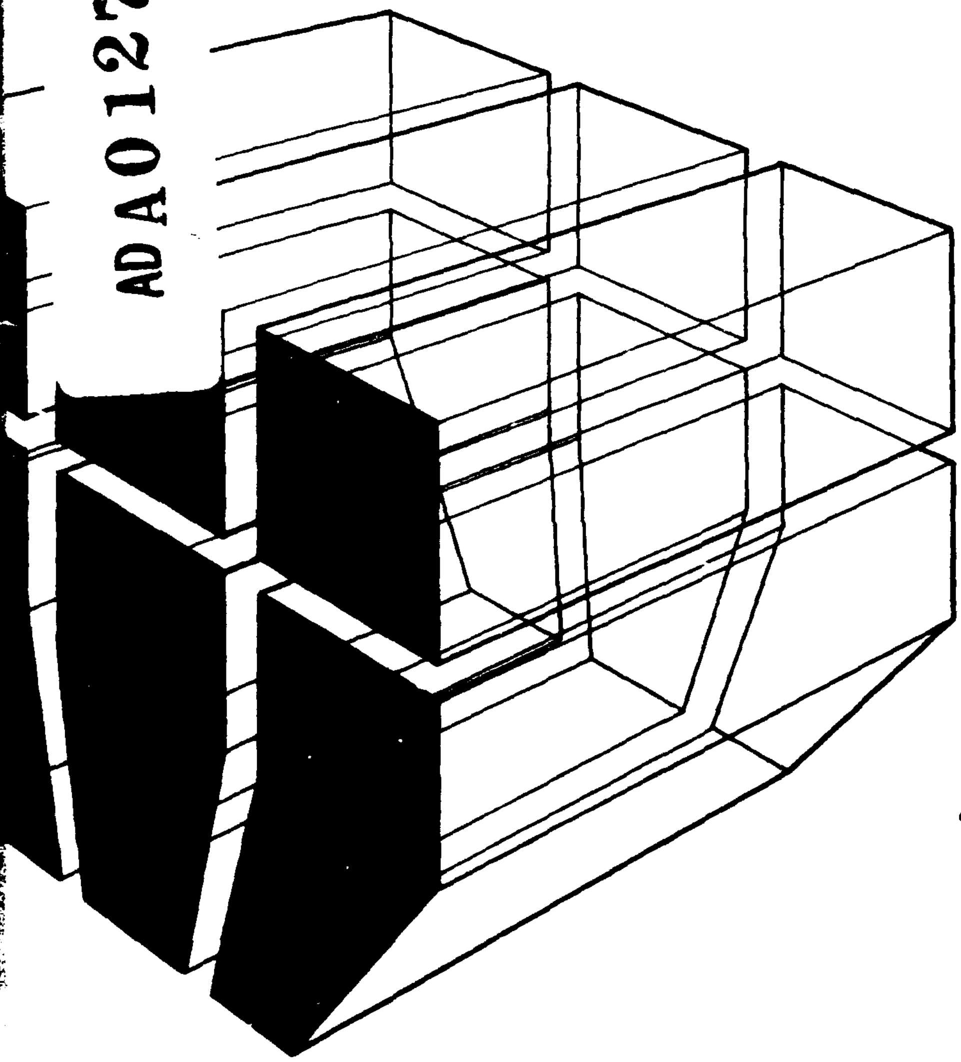

by
D. J. Leverenz
P. H. Nielsen
R. G. McCormack

CERL

Approved for public release; distribution unlimited.

UNCLASSIFIED

SECURITY CLASSIFICATION OF THIS PAGE (When Data Entered)

REPORT DOCUMENTATION PAGE

READ INSTRUCTIONS BEFORE COMPLETING FORM

1. REPORT NUMBER: 14 CERL-TR-C-19
2. GOVT ACCESSION NO.
3. RECIPIENT'S CATALOG NUMBER

4. TITLE (and Subtitle): 6 EMP SHIELDING PROPERTIES OF CONDUIT SYSTEMS AND RELATED HARDWARE.

5. TYPE OF REPORT & PERIOD COVERED: 9 FINAL RE[redacted]T,

6. PERFORMING ORG. REPORT NUMBER

7. AUTHOR(s): 10 D. J./Leverenz, P. H./Nielsen, R. G./McCormack

8. CONTRACT OR GRANT NUMBER(s): ~~IAO 72-20~~

9. PERFORMING ORGANIZATION NAME AND ADDRESS:
CONSTRUCTION ENGINEERING RESEARCH LABORATORY
P.O. Box 4005
Champaign, IL 61820

10. PROGRAM ELEMENT, PROJECT, TASK AREA & WORK UNIT NUMBERS

11. CONTROLLING OFFICE NAME AND ADDRESS

12. REPORT DATE: 11 Jun[redacted]75 12 102p.

13. NUMBER OF PAGES: 102

14. MONITORING AGENCY NAME & ADDRESS (if different from Controlling Office)

15. SECURITY CLASS. (of this report): Unclassified

15a. DECLASSIFICATION/DOWNGRADING SCHEDULE

16. DISTRIBUTION STATEMENT (of this Report)

Approved for public release; distribution unlimited.

17. DISTRIBUTION STATEMENT (of the abstract entered in Block 20, if different from Report)

18. SUPPLEMENTARY NOTES

19. KEY WORDS (Continue on reverse side if necessary and identify by block number)

conduit runs
EMP fields
SAFEGUARD

405279

20. ABSTRACT (Continue on reverse side if necessary and identify by block number)

This report presents the results obtained by CERL over the past 3 years under its investigation of the shielding properties of conduit systems, conduit-related hardware, and the effects of improper field assembly on the shielding of conduit systems. The measurements were made by injecting EMP-type current pulses onto test conduits and measuring the signal picked up on a sense wire inside the conduit.

Results are presented for the measurement of both diffusion and → OVER

DD FORM 1473, 1 JAN 73 EDITION OF 1 NOV 65 IS OBSOLETE

UNCLASSIFIED

SECURITY CLASSIFICATION OF THIS PAGE (When Data Entered)

Block 20 continued.

leakage signals. The diffusion signal provides a base line for the conduit shielding since it is the optimum shielding obtainable for a given size and material of conduit. The leakage signals represent a degradation of the conduit shielding due to the insertion of conduit hardware required to assemble the conduit runs, or to the improper assembly of the conduit system.

Included in the leakage study were various hardware items including couplings, unions, conduits of various sizes, flexible conduit, condulets, lock nuts, threaded hubs, and a variety of condulet gaskets. In addition, the effects of thread corrosion, use of different conductive compounds, various methods of compound application, welding near couplings, and the inadequate tightening of threaded joints were evaluated.

The greatest single factor in the degradation of the shielding effectiveness of conduit assemblies was the inadequate tightening of conduit joints. Rusted threads also caused a considerable degradation of shielding effectiveness, but this was considerably lessened when the conduit joints were properly tightened. The use of conductive compounds was found to have only a minimum effect on shielding effectiveness. If properly installed, most hardware items caused little shielding degradation.

FOREWORD

This investigation was conducted for the U. S. Army Engineer Division, Huntsville (HND), under IAO 72-20, dated 2 August 1971 and subsequent change orders. The work was performed by the Facilities Engineering and Construction Division (FE) of the U. S. Army Construction Engineering Research Laboratory (CERL).

COL M. D. Remus is the Commander and Director of CERL and Dr. L. R. Shaffer is the Deputy Director. Mr. E. A. Lotz is Chief of FE.

Appreciation is expressed to Dr. J. Verdeyen and M. J. Pollock for their guidance, and to L. Greep, M. Hill, W. Croisant, D. Seiber, E. Spier, and T. Tuttle, of CERL, for their assistance in the conduct of this investigation. Appreciation is also expressed to F. Smith and M. Carter of Huntsville (HND) for their suggestions.

CONTENTS

DD FORM 1473 1
FOREWORD 3
LIST OF FIGURES AND TABLES 5

1 INTRODUCTION 11
Problem
Background
Purpose

2 TEST PROCEDURES 13
Test Facility
Instrumentation

3 CONDUIT DIFFUSION SIGNALS 19
Introduction
Background
Experimental Procedure
Test Results
Conclusions

4 CONDUIT LEAKAGE SIGNALS DUE TO POOR COUPLING ASSEMBLY 30
Introduction
Background
Experimental Procedure
Test Samples
Rusting and Aging of Conduit Samples
Test Results
Conclusions

5 CONDUIT LEAKAGE CURRENT FROM CONDUIT RELATED HARDWARE 55
Introduction
Experimental Procedure
Test Sample Preparation
Test Results
Conclusions

DISTRIBUTION

FIGURES

Number		Page
1	Block Diagram of Parallel Conduit Transmission Line	14
2	Conduit Current on Ground Side of Transmission Line	15
3	Time Domain Reflectometer Display for Conduit Transmission Line	15
4	Current Injection End Cap with Sense Wire Attached	16
5	One-In. Parallel Conduit Transmission-Line Test Setup Attached to a Shielded Enclosure	17
6	Stoddard (Singer-Gertsch) Model 95162-4, Current Probe, Twin-Ax, and Balun Frequency Response	18
7	Adelco Model MMO-5286-2, Current Probe, Balun, and Avantek Amplifier Frequency Response	20
8	Response of Adelco Current Probe and Balun to 100 kHz Square Wave	21
9	Experimental Setup	26
10	Typical Conduit Pulse--Voltage Drop Measured Across the Transmission-Line Termination Resistor	27
11	Diffusion Signal for 1-In. Galvanized Steel Conduit Showing Sense Wire Voltage	28
12	Diffusion Signal for 2-In. Galvanized Steel Conduit Showing Sense Wire Voltage	29
13	Demonstration of Impulse Response	31
14	Sense-Wire Short-Circuit Current	35
15	Environmental Chamber for Rusting and Aging Conduit Samples	38
16	Typical Set of Oscilloscope Pictures	41
17	Test Sample of 4-In. Explosion-Proof Union Installed on Conduit Sections	56
18	Standard 2-In. and Modified 1-In. UNF Unions Showing Flat-Mating Surfaces	57

FIGURES (cont'd)

Number		Page
19	One-In. Explosion-Proof Union (UNY) Installed in Transmission Line	57
20	Four-In. Conduit Sample Being Assembled Using Pipe Wrench and Extensions	59
21	Non-RFI Tight Flexible Conduit Sample (Sealtite) Without Ground Wire	61
22	Non-RFI Tight Flexible Conduit Sample (Sealtite) With Ground Wire	61
23	PVC-Covered 1 1/2-In. RFI Tight Flexible Conduit Sample as Installed in the Parallel Conduit Transmission Line (Showing Reducers)	62
24	PVC-Covered 1 1/2-In. RFI Tight Flexible Conduit Sample as Installed in the Parallel Conduit Transmission Line	62
25	A 1 1/2-In. Flexible Conduit Sample with a Standard Steel Flexible Bellows and Two Layers of Galvanized Steel Braid	63
26	A 4-In. Flexible Conduit Sample with a Standard Steel Flexible Bellows and One Galvanized Steel Braid	63
27	A 4-In. Flexible Conduit Sample with a Standard Steel Flexible Bellows and One Galvanized Steel Braid with a 1-In. Wide Tinned Copper Braid in Parallel with the Flexible Section	65
28	A 1 1/2-In. Flexible Conduit Sample with a Hypermaflex Flexible Bellows and One Stainless-Steel Braid with Braid Intact	65
29	A 1 1/2-In. Flexible Conduit Sample with Hypermaflex Flexible Bellows and One Stainless-Steel Braid, Showing the Braid Disconnected from One End	66
30	A 1 1/2-In. Flexible Conduit Sample with Hypermaflex Flexible Bellows After the Stainless-Steel Braid Had Been Removed	66
31	Specially Designed 1 1/2-In. Flexible Conduit Sample with Hypermaflex Flexible Bellows and One Galvanized Steel Braid	67

FIGURES (cont'd)

Number		Page
32	Specially Designed 1 1/2-In. Flexible Conduit Sample Showing the Automotive Screw-Type Hose Clamp Used to Secure One End of the Galvanized Steel Braid	67
33	Condulet Test Samples	68
34	Summary of Combination of Condulets, Gaskets, and Covers Tested	69
35	Type 35C Condulet with 11-Gauge Steel Cover and Three U-Bolts	71
36	Type 35C Condulet with 11-Gauge Steel Cover and Steel Shipping Bands	71
37	Heated Coupling Sample Shown After Having Been Heated	72
38	Rusted 2-In. Conduit Sample as Installed in Parallel Conduit Transmission Line (Showing Reducer)	73
39	Lock-Nut Test Samples	75
40	Close-Up of Lock-Nut Test Assembly	75
41	Exploded View of Threaded-Hub Test Sample	76
42	Close-Up of Threaded-Hub Test Assembly	76
43	Cut-Away End View of Transmission Line Showing Orientation of Slot for Transverse-Slotted Conduit Tests	78
44	Three-Ft Long Sample as Installed	80
45	Four-Ft Long Sample as Installed	80
46	I_{sc} Wave Form--1 1/2-In. Flexible PVC-Covered Conduit	87
47	I_{sc} Wave Form--4-In. Standard Steel Flexible Bellows with Galvanized Steel Braid	87
48	I_{sc} Wave Form--1 1/2-In. Hypermaflex Bellows with Double-Galvanized Steel Braid	88
49	I_{sc} Wave Form--1 1/2-In. Hypermaflex Bellows with Double-Galvanized Steel Braid	88

FIGURES (cont'd)

Number		Page
50	I_{sc} Wave Form--1 1/2-In. Special Design Flexible Conduit	89
51	I_{sc} Wave Form--1 1/2-In. Special Design Flexible Conduit	89
52	I_{sc} Wave Form--1-Ft Conduit Length	100
53	I_{sc} Wave Form--1-Ft Conduit Length	100
54	I_{sc} Wave Form--11-Ft Conduit Length	101
55	I_{sc} Wave Form--11-Ft Conduit Length	101

TABLES

1	Conduit Diffusion Signal Test Results	25
2	Test Samples of 1-In. Conduit	36
3	Conduit Test Data	44
4	Summary of Explosion-Proof Union Test Combinations	58
5	Summary of 4-In. Conduit Couplings Test Combinations	59
6	Explosion-Proof Union Test Data	82
7	Test Results Using 4-In. Conduit Couplings	83
8	Interior Non-RFI Tight 1-In. Flexible Conduit Test Data	84
9	Test Results Using RFI-Tight Flexible Conduit	86
10	Results of Tests on Condulets, Covers, and Gaskets	90
11	Heated Coupling Test Data	92
12	Results of Tests Using Rusted 2-In. Conduit--Field Rust vs Laboratory Rust	93
13	Results of Repeatability Tests Using Rusted 1-In. Conduit	94
14	Results of Shielding-Effectiveness Tests of 1-In. Threaded Hubs	95
15	Results of Shielding-Effectiveness Tests of 1-In. Lock Nuts	96

TABLES (cont'd)

Number		Page
16	Results of Tests Using Transverse-Slotted Conduit	97
17	Results of Tests Using Differential-Mode Sense Wires	99
18	Results of Tests Using Various Lengths of Conduit	102

EMP SHIELDING PROPERTIES OF CONDUIT SYSTEMS AND RELATED HARDWARE

1 INTRODUCTION

Problem. The Huntsville Engineering Division, HND, has requested that CERL investigate the shielding properties of conduit systems, particularly the degradation in shielding that occurs due to the use of different types of conduit hardware and the effects of nonstandard conduit-coupling conditions.

Background. A considerable effort has been made to protect the SAFEGUARD site from damage due to the effects of the nuclear electromagnetic pulse (EMP). As part of EMP protection, large volumes of the SAFEGUARD structures that house critical and vulnerable electronic equipment and circuits have been completely enclosed in a continuous steel shell. This shell is designed to attenuate the EMP fields to a level that electronic equipment can tolerate without degradation in performance. An integral part of this EMP-shielding system is the conduit runs that carry the instrumentation and power cables between the shielded structures.

The conduit used at the SAFEGUARD site is rigid-wall galvanized steel 10 ft in length, and varies from 1 to 8 in. in diameter. Steel rigid-wall conduit was used because it provides shielding equivalent to or greater than that provided by the steel liner plate used to construct the shielded volume for the electronic equipment. Because of the long runs of conduit, the need to provide a means for pulling the cables, and the requirements for shock isolation, such hardware items as couplings, unions, pull boxes, junction boxes, condulets, and flexible conduits were used to join the 10-ft sections of conduit. Thus a conduit run, since it is not completely continuous and uniform, can have defects resulting in possible EMP leakage and degradation of shielding effectiveness. Unfortunately, the amount of degradation caused by the various hardware items is not known and thus evaluation of overall conduit-system shielding effectiveness is not possible. Even where an item is known to provide good EMP shielding, improper installation of the item onto the conduit run can cause a degradation in shielding.

The specified procedure for assembling the hardware items in the conduit runs requires that the conduit threads be brushed clean with a wire brush and that a coating of conductive compound be applied before joining with the mating thread on the hardware item. The joint is then assembled and securely tightened with a pipe wrench. Where conduit runs enter a shielded volume, they are to be welded to the steel liner plate. These precautions are taken to insure that shielding integrity is maintained.

Due to the vast amount of conduit which is installed at the SAFEGUARD site, there can be situations when this assembly procedure is not followed--such as corrosion of the threads, especially on conduits that have been threaded in the field; improper tightening of the conduit couplings; and improper application of conductive compound. The effects of these installation conditions on the EMP shielding of the conduit runs is unknown; therefore, it is not possible to determine whether these conditions must be corrected. This information is often critical since considerable amounts of conduit are buried and repair can be expensive and time-consuming.

For these reasons, HND has requested that CERL determine the shielding properties of various conduit hardware items, and where several methods of installation are possible, determine the best alternative. In addition, CERL was requested to investigate the effects of various coupling conditions on conduit-shielding effectiveness, so that such information would be available to determine the necessity of corrective measures.

In addition to determining whether corrective action is required, this investigation will assist HND, the SAFEGUARD System Command (SAFSCOM), and the weapon system contractor (WSC) in:

a. Evaluating the overall SAFEGUARD site EMP-shielding effectiveness;

b. Determining the levels of EMP signals that the electronic equipment must be able to withstand; and

c. Deciding whether a full-threat level site test of the EMP shield is necessary.

Purpose. EMP fields will induce a current pulse on the outside of the conduit system. This pulse will in turn induce currents on the cables inside the conduit.

The purpose of this investigation is to determine the common-mode signal induced on a wire inside the conduit by a known current flowing on the conduit (for a variety of conduit configurations).

The base-line for the shielding that can be provided by the conduit is the diffusion current that penetrates the conduit itself. The value of the diffusion current thus is related to maximum shielding effectiveness possible from the conduit.

Leakage current results from imperfections in the conduit run. Studies were made of leakage through couplings, in particular, the leakage with regard to coupling installation condition (i.e. rusted threads, loose connection, etc.) and the leakage resulting from the insertion of various pieces of conduit hardware. Since the experimental

setup is essentially the same for the three areas of the test, this report begins with a description of the setup and the instrumentation used for measuring the sense-wire signal.

2 TEST PROCEDURES

Test Facility. The conduit-shielding investigations were conducted at CERL in a test setup shown schematically in Figure 1. This setup includes a 50 kV fast-rise time pulser, a parallel-pipe transmission line terminated in its characteristic impedance, and a shielded enclosure.

The pulser consists of a low-inductance cylindrical capacitor (typically .02 μF) and a spark gap mounted coaxially inside a cylindrical chamber. The chamber is air-tight and can be pressurized with sulfahexafluoride (SF_6). The pulser is supplied by a 50 kV DC power supply. The firing voltage is controlled by the spark gap spacing and gas pressure. In operation, the capacitor is charged by the DC power supply until the voltage necessary to fire the spark gap is reached. When the spark gap fires, the capacitor is discharged into the pulser load and the capacitor starts to recharge. The pulser is thus free-running with the repetition rate controlled by the amount that the voltage of the DC supply exceeds the firing voltage of the spark gap. With a 200-ohm transmission-line load, it was possible to get an output pulse with a rise time of 3 nsec, a fall time (e-fold) of 4 μsec and a repetition rate of 1 pulse/sec. Typically, the DC voltage supply was set for 38 kV with the spark gap set to fire at 30 kV. This provided a 150-amp peak current pulse approximately every 2 sec. This output current pulse is shown in Figure 2. This current was measured on the ground side of the transmission line with the Stoddard current probe, described later in this chapter.

The load for the pulser was a parallel conduit transmission line, formed by two parallel sections of rigid-wall galvanized-steel conduit (generally, 10-ft sections of 1 in. conduit were used). One end of the transmission line was connected to the pulser through special low-inductance end caps attached to the end of the conduit sections. The other end of the line was terminated with a load resistor. This load resistor was generally chosen to be the characteristic impedance of the line (typically 200 ohms). The matched transmission line thus provided a resistive load for the pulser which produces a double-exponential output current pulse on the transmission line. Figure 3 shows the time-domain reflectometer measurement of the 200-ohm matched transmission line.

A conduit assembly including the hardware item or prepared coupling was used as the ground side of the transmission line. This test conduit extended beyond the terminating resistor and screwed into a conduit stub that had been welded into the side of a shielded enclosure. A sense wire (12-gauge solid copper) was connected to the inside of the end cap of the test conduit (Figure 4) at the pulser end of the transmission

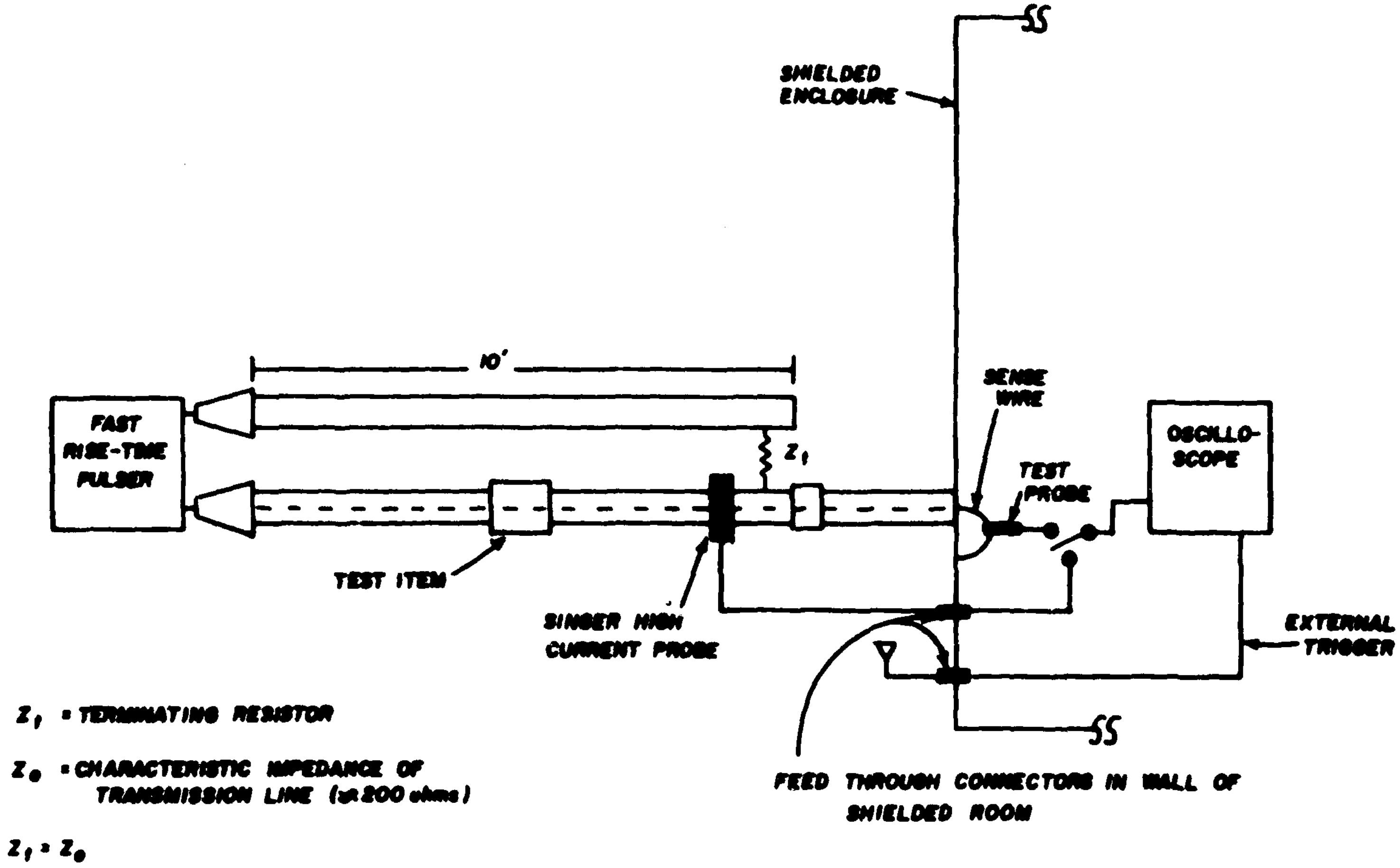

Figure 1. Block diagram of parallel conduit transmission line.

Figure 2. Conduit current on ground side of transmission line (vertical scale, 50 amp/div; horizontal scale, 0.5 μsec/div).

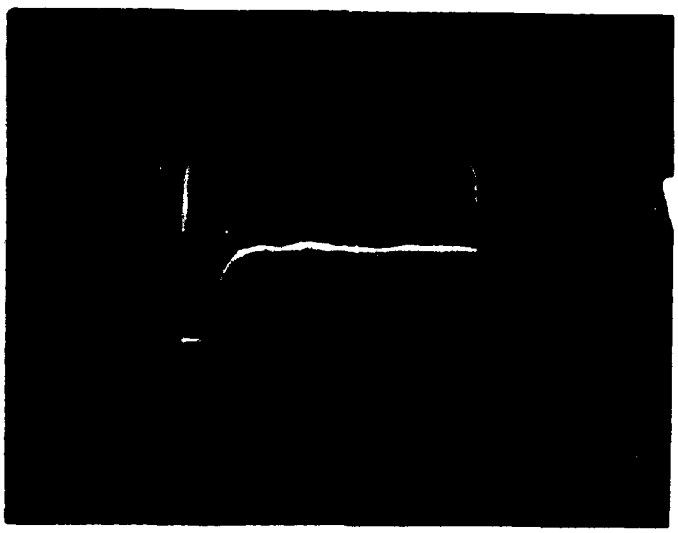

Figure 3. Time domain reflectometer displays for conduit transmission line (Z_t, 200 ohm; vertical scale, 5 mV/div; horizontal scale, 10 nsec/div).

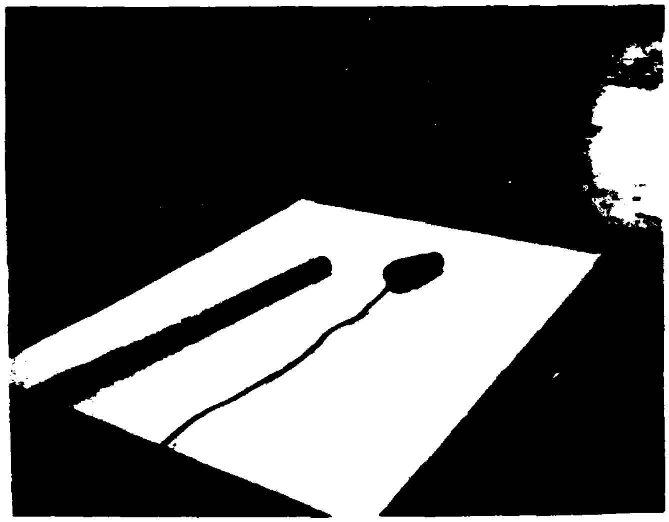

Figure 4. Current injection end cap with sense wire attached.

line, and routed through the test sample and conduit stub and into the shielded chamber where the voltage and current measurements were taken. The sense wire could be terminated at either end in impedances R1 and R2, depending on the test under consideration. In general, R1 was 0 (i.e. short circuit) and R2 was 0, 100Ω, or ∞ (open circuit). Measurements were generally taken of I_s, the current through R2, and/or Vs, the voltage across R2. The majority of the data is reported for the short-circuit current (I_s for R2=0) which is labeled I_{sc}.

Several shielded enclosures were used to house the instrumentation. In some cases a screen room was used, and in others one of two all-welded 11-gauge steel chambers was used. In either case the room used provided adequate electromagnetic shielding from the pulser and other external noise sources to provide an accurate measurement of the sense-wire signal.

In order to attach the test conduit to the shielded enclosure, a conduit stub was welded into a hole in a side of the chamber. A coupling was welded to the end of this conduit and this formed the stub to which the conduit samples were connected. Power for inside the shielded room was brought in through power-line filters. A twin-ax feed-through was installed in the wall of the enclosure to connect the Stoddard current probe to an oscilloscope inside the shielded room. This probe was used to measure the current flowing on the transmission line. A BNC feed-through was used to connect the oscilloscope trigger to a small-monopole antenna outside the enclosure. In this way, radiation from the pulser provided a trigger signal for the measuring equipment.

The test setup described in this section provided the means for injecting the 150-amp current pulse shown in Figure 2 onto the outside of

the test conduit sample; and the apparatus for measuring the pickup on the sense wire inside the conduit while protecting the measuring equipment from electromagnetic interference. A typical setup is shown in Figure 5.

Instrumentation. The data taken for the studies reported herein included oscilloscope photographs of the following: current on the conduit, current on the sense wire, and voltage across the sense-wire termination. Initially all three were taken. However, since the I_{sc} measurement was primarily the one used for comparing the performance of the various test items, it was the only measurement made for some tests.

Conduit Current Measurement. The current flowing on the conduit transmission line is determined by the pulser and transmission-line characteristics. Typically, it is a double-exponential current pulse with a 3 nsec rise time and a fall time of about 4 μsec. Since this current is the driving force for the sense-wire current, it was monitored for all tests. The probe which was used to measure this current was a Stoddard Model 95162-4. This probe is a balanced, shielded design, using a split-toroidal coil which can be opened for placement onto the test conduit. The probe has the following characteristics:

- Transfer impedance--0.1 ohm nominal (10 volts into 125-ohm load for 1-amp signal).

- Frequency response--flat within ± 1 dB from 5 kHz to 100 MHz with upper and lower 3 dB frequencies of 120 MHz and 2.4 kHz, respectively. The low-frequency content of observed signals is influenced by the combined response, of the probe, twin-ax, and balun. This combined low-frequency response was measured and is shown in Figure 6.

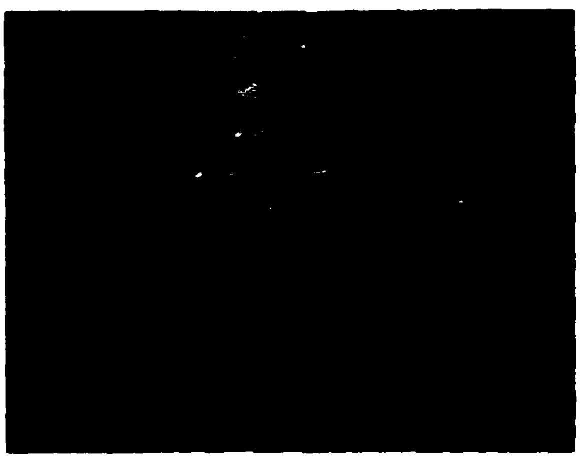

Figure 5. One-in. parallel conduit transmission-line test setup attached to a shielded enclosure.

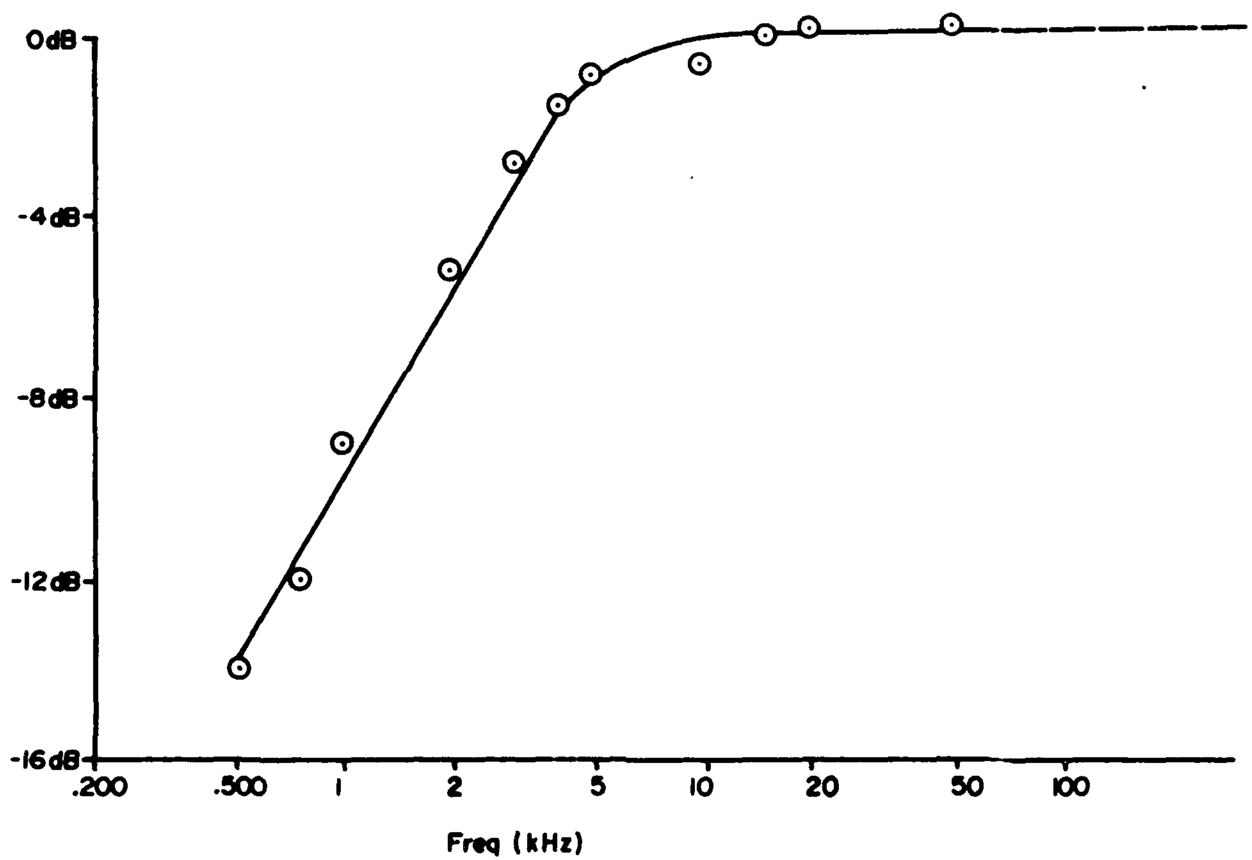

Figure 6. Stoddard (Singer-Gertsch) model 95162-4, current probe, twin-ax, and balun frequency response.

Sense-Wire Measurements. The sense wire, which was contained within the conduit sample, was connected internally to the end cap and protruded into the shielded enclosure. During tests, the sense wire was terminated inside the shielded enclosure adjacent to the base of the conduit stub. For short-circuit current tests, the sense wire was grounded by means of a heavy, copper-ground lug/clamp assembly soldered to the enclosure wall. Voltage-load and current-load tests were performed with the sense wire terminated into an appropriate resistor. One end of the resistor was soldered to the enclosure wall adjacent to the welded conduit stub. The other end was connected to the sense wire by means of a standard alligator clip. For the open-circuit voltage tests, no sense-wire termination was used.

Several current probes were used to measure the sense-wire current. Where maximum sensitivity was required, an Adelco Model 52896-2 (formerly made by Martin Marietta) current probe was used with a balun and an Avantek wide-band low-noise amplifier. The probe has a transfer impedance of 1.94 ohms nominal and 3 dB frequencies of 20 kHz and 200 MHz. A plot of the combined low-frequency response of the probe, balun, and wide-band amplifier is shown in Figure 7. The wide-band amplifier had a gain of 50 dB and was used for low-level signals only. Its response, however, was much broader than the probe and balun combination; hence, the low-frequency content of observed pulses was not appreciably affected by the amplifier. Oscilloscope photographs of the probe and balun response to a 100-kHz square wave are shown in Figure 8. As evidenced by the photograph, considerable droop of the signal occurs within the observed 5 μsec period. The fall times observed in conduit test data must be corrected accordingly.

Because of the poor low-frequency response of the Adelco probe, much of the data was taken using the Tektronix P6021 or P6022 current probe. Depending on whether the termination was passive or active, these probes had a low-frequency response of 1 kHz and 10 Hz, respectively. Thus, an accurate measurement of the sense-wire current, including low-frequency content, was obtained. Since the Tektronix probes were 10 times less sensitive than the Adelco probe, it was necessary to use the Adelco probe for most of the coupling-condition studies. The Tektronix probes, however, were used for most of the hardware items study.

The voltage across the sense-wire termination was measured using standard Tektronix voltage probes. Single-ended and balanced probes were compared and no appreciable difference was noted. In no case was the frequency response of the voltage probe found to affect the data.

3 CONDUIT DIFFUSION SIGNALS

Introduction. In analyzing the electromagnetic shielding provided by conduit systems, the direct diffusion of the external signal through

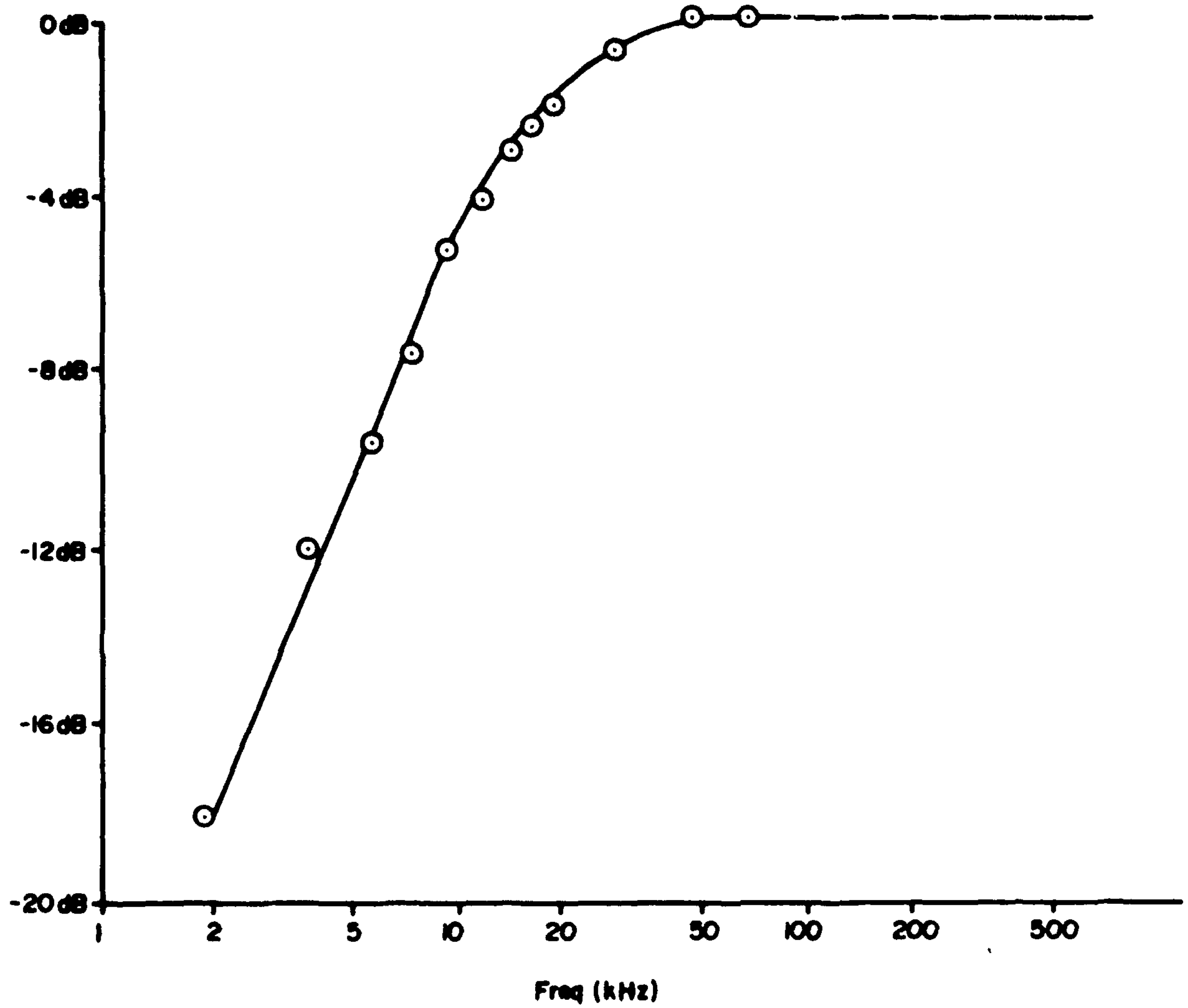

Figure 7. Adelco model MMO-5286-2, current probe, balun and Avantek amplifier frequency response.

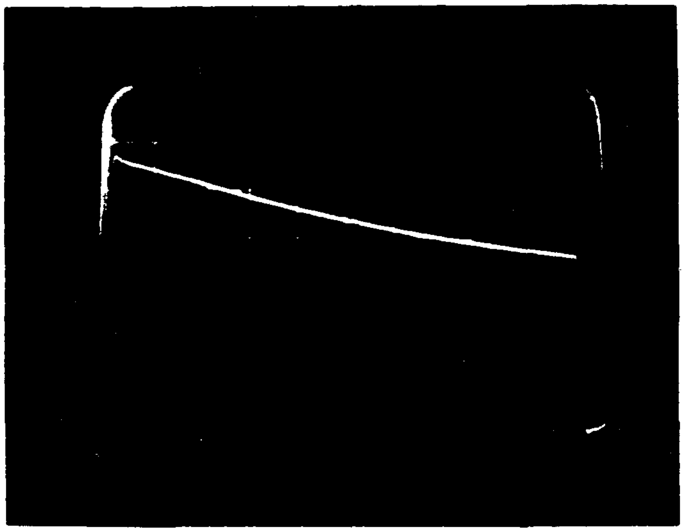

Figure 8. Response of Adelco current probe and balun to 100 kHz square wave (vertical scale, 5 mV/div; horizontal scale, 0.5 μsec/div).

the conduit is important. These diffusion signals, unlike the leakage signals that penetrate through holes or flaws in the conduit system, are due to the conduit's finite-shielding capability. The strength of these diffusion signals depends on the conduit material and size and the frequency content of the external radiation. Thus, for a given external excitation, the diffusion signal is a function of the conduit itself and defines a base line or maximum-shielding level that can be obtained for a given conduit system.

Background. The diffusion-signal phenomenon has a firm foundation in electromagnetic theory, and the analytic treatment provides a basis for predicting these diffusion signals when such variables as conduit material, size, length, and surface current are known. Electromagnetic fields induced by the surface current can be thought of as diffusing through the conduit wall and inducing voltages and currents on the wires inside the conduit. Because the diffusion process is highly frequency dependent, the shape of the signal induced on the wires inside the conduit can be radically different from the existing current on the outside of the conduit. The diffusion process has many characteristics of a low-pass filter, and thus most of the high-frequency energy in the existing current is attenuated. In many cases, the conduit current will have decayed to a very low value before the diffusion signal has reached an appreciable magnitude. This pulse is narrow enough to appear to the diffusion signal as an impulse. Thus, the diffusion signals measured using the experimental setup are, for practical purposes, the diffusion-signal impulse response, $v_I(t)$, of the conduit system.

Once this impulse-response voltage is known, the induced voltage on the sense wire v(t) for any conduit-driving current $I_c(t)$ can be found from the convolution integral

$$v(t) = \int_0^t v_I(t-\lambda)\ I_c\ (\lambda)\ d\lambda. \qquad \text{[Eq 1]}$$

To use Eq 1, however, $v_I(t)$ must be the response to a unit-impulse driving current. Although the wave shape of the impulse-diffusion signal is, for practical purposes, independent of the wave shape of the impulse current applied to the conduit (i_c), the magnitude of the impulse-diffusion signal is not independent of the injected current, but depends on the total charge injected onto the conduit. Since the integral of the unit-impulse current over all time is one, and the integral of the impulse current for the experimental setup is the total charge, Q, on the capacitor in the pulser

$$Q = cv \qquad \text{[Eq 2]}$$

where

$$c = .02\ \mu f \qquad \text{[Eq 3]}$$

$$v = \text{pulser firing voltage.} \qquad \text{[Eq 4]}$$

The experimental conduit current $I_c(t)$ can be assumed, for diffusion current measurements, to be

$$I_c(t) = Q\ \delta(t) \qquad \text{[Eq 5]}$$

where $\delta(t)$ is the Dirac Delta function (an impulse with an area of 1 with infinite height and 0 width). Thus, the voltage measured on the sense wire, $v_m(t)$, using the experimental setup, will be from Eq 1 and Eq 5

$$v_m(t) = v_{I(t)}\ Q. \qquad \text{[Eq 6]}$$

To determine the sense-wire current I(t) from the sense-wire voltage calculated in Eq 1, the sense-wire circuit must be considered as being driven by the voltage v(t). Since the coupling between the external-conduit current and the sense-wire current is negligible, the induced voltage on the sense wire will be independent of the sense-wire current and the sense-wire loading. Therefore, v(t) can be thought of as a constant voltage source. Unlike the leakage signals that occur in the nanosecond region, the diffusion current in galvanized-steel conduits is on the order of milliseconds; thus, the transmission-line properties of the sense wire inside the conduit are relatively unimportant (except for extremely long conduit systems). Therefore, the sense wire inside the conduit can be treated as a lumped parameter system and the sense-wire current can be obtained from the equation

$$I(t) = \frac{V(t)}{R_{total}} \qquad \text{[Eq 7]}$$

where R_{total} is the total resistance of the sense-wire conduit system, including any sense-wire load resistance. Also, since the diffusion occurs along the entire length of the conduit, the diffusion signal will increase linearly with conduit length. Thus, the induced voltage per unit length v(t) can be found from

$$v^*(t) = \frac{v(t)}{\ell} \qquad \text{[Eq 8]}$$

where ℓ is the length of the conduit. Using the experimental setup of Chapter 2, the impulse response per unit length, $v_I^*(t)$, can be determined from Eq 6 and 8 as

$$v_I^*(t) = \frac{v_m(t)}{Q\ \ell} \qquad \text{[Eq 9]}$$

From $v_I^*(t)$, the diffusion voltage, v(t), and current, I(t), on a sense wire for any given conduit current $I_c(t)$, can be found from

$$v(t) = \ell_c \int_0^t v_I^*(t - \lambda) I_c(\lambda) d\lambda \qquad \text{[Eq 10]}$$

and

$$I(t) = \frac{v(t)}{R_{total}} \ . \qquad \text{[Eq 11]}$$

For convenience, $v_I^*(t)$ can be given as

$$v_I^*(t) = M\ v_I^{*n}(t) \qquad \text{[Eq 12]}$$

where $v_I^{*n}(t)$ is $v_I^*(t)$ normalized to a peak value of 1. This chapter gives the experimentally determined values for M and $v_I^{*n}(t)$.

Experimental Procedure. The study of conduit-diffusion signals was made on solid 10-ft sections of rigid-wall, galvanized steel conduit to examine the maximum electromagnetic shielding level that can be obtained with such a conduit.

The test setup is essentially the same as that described in Chapter 2, with only minor instrumentation modifications. Standard 10-ft sections of both 1- and 2-in. rigid-wall, galvanized steel were tested. The ends were cleaned with a power wire brush and coated with Chomerics 4331 conductive compound to insure that no leakage signal entered the conduit.

An end cap with the sense wire attached was wrench-tightened onto one end of the test sample. The other end of the test sample was wrench-tightened onto the conduit stub that had been welded to the shielded chamber. The sense wire was pulled through the conduit and extended into the shielded chamber. After installing the test sample as the ground side of a parallel-transmission line, the remainder of the transmission line was assembled, the pulser was connected, and the sample was tested.

The transmission line was terminated in its characteristic impedance of 200 ohms, and the pulser was set to fire at 30 kV. Thus the pulser produced a 150-amp peak current pulse with a rise time of less than 10 nsec, and a fall time (e-fold) of 4 μsec. This current pulse was monitored by measuring the voltage drop across the transmission-line termination resistor using a Tektronix P-6015 high-voltage probe.

Because of the large amounts of low-frequency energy contained in the diffusion signal, it was not possible to accurately measure the short-circuit sense-wire current since the current probes suitable for the leakage measurements did not have an adequate low-frequency response for measuring diffusion currents. Therefore, the voltage across the sense-wire termination resistor was measured using an operational amplifier whose output was connected directly to the oscilloscope. This voltage sensing device (Figure 9) had a low-frequency response that was flat to 0 Hz.

Test Results. Test results are shown in Table 1 and were obtained from the oscilloscope photos shown in Figures 10, 11(a) and (b), and 12(a) and (b). These pictures include:

a. The voltage drop across the transmission-line termination resistor for a conduit current pulse (Figure 10);

b. The sense-wire voltage showing the diffusion signal rise time of the 1-in. conduit (Figure 11(a)) and the 2-in. conduit for a current pulse similar to the one shown in a. above (Figure 12(a));

c. The sense-wire voltage showing the diffusion signal fall time for the 1-in. conduit (Figure 11(b)) and the 2-in. conduit for a current pulse similar to the one shown in a. above (Figure 12(b)).

To demonstrate that the pulse being used was sufficiently short to be termed an impulse, pulses of the form

$$Ic(t) = I_o e^{-t/\tau} \qquad \text{[Eq 13]}$$

where

$Io = \frac{V}{R}$

V = the firing voltage of the pulser

R = transmission-line termination resistance

and

τ = RC

C = capacitance of the pulse

Table 1

Conduit Diffusion Signal Test Results

Size Conduit	Time to Peak	Time from Peak to 1/e	$M_{\frac{volt}{ft\text{-}coulomb}}$*	V_{volt}**
1 in.	1.5 msec	2.1 msec	4.2×10^{-2}	2.5×10^{-4}
2 in.	2.2 msec	3.3 msec	1.6×10^{-4}	6.8×10^{-5}

* M is given in Eq 12 and is the peak sense-wire voltage induced per foot of conduit per coulomb of charge injected on the conduit.

** V is the peak voltage induced on a 10-ft conduit-sense wire due to a current pulse with a 150-amp peak current and a 4 μsec fall time (6.0×10^{-4} coulomb of charge).

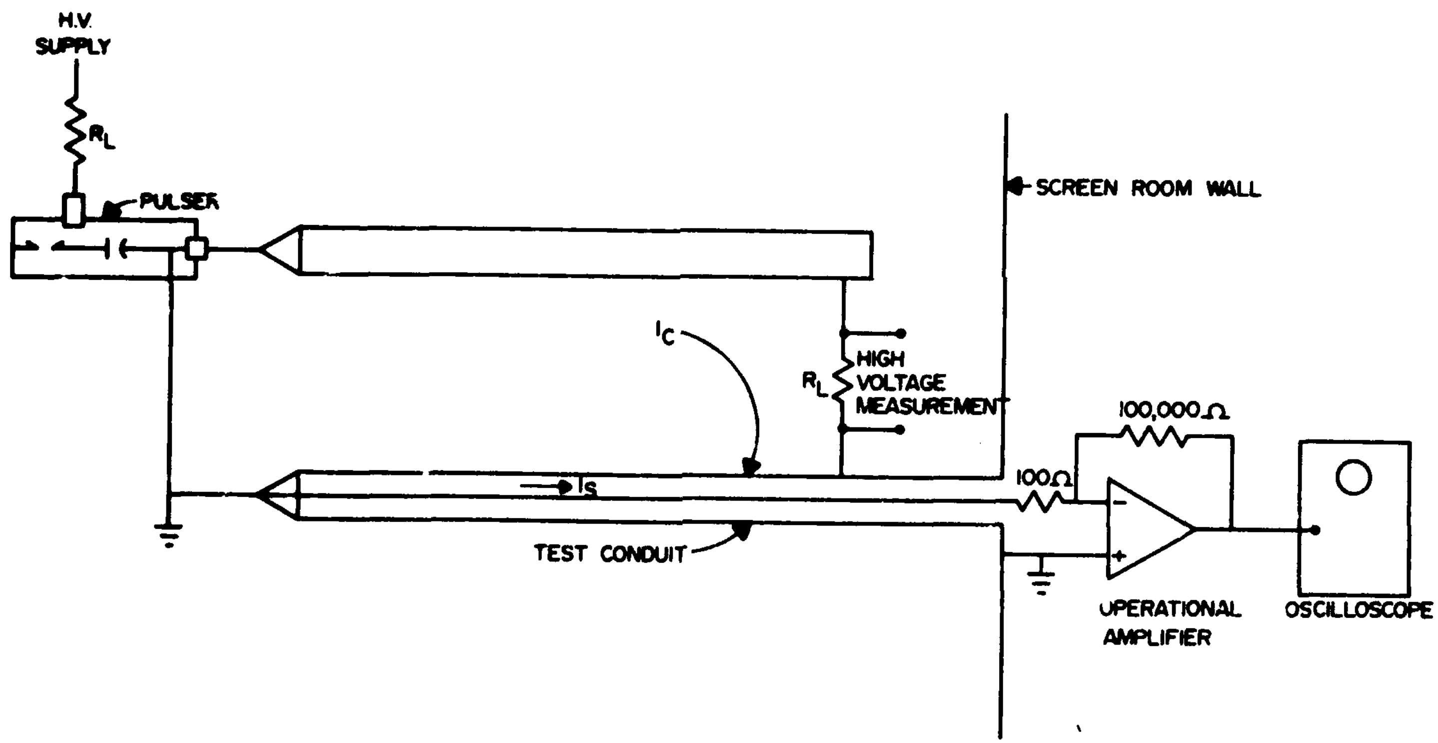

Figure 9. Experimental setup.

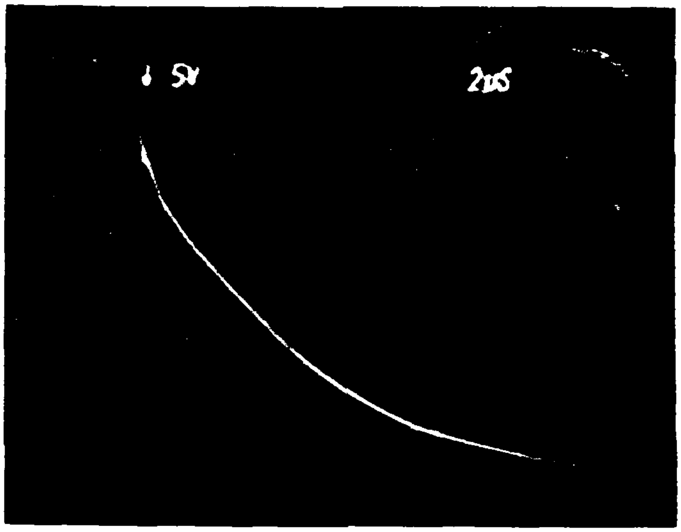

Figure 10. Typical conduit pulse--voltage drop measured across the transmission-line termination resistor (scale: 5000 V/division, vertical; 2μsec/division, horizontal).

(a) Vertical: 1000 x 50 mV/div
Horizontal: 200 μsec/div

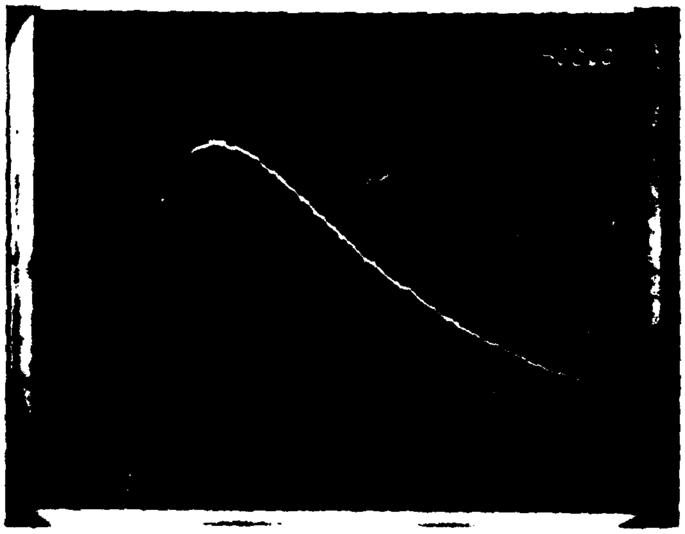

(b) Vertical: 1000 x 50 mV/div
Horizontal: 500 μsec/div

Figure 11. Diffusion signal for 1-in. galvanized steel conduit showing sense wire voltage.

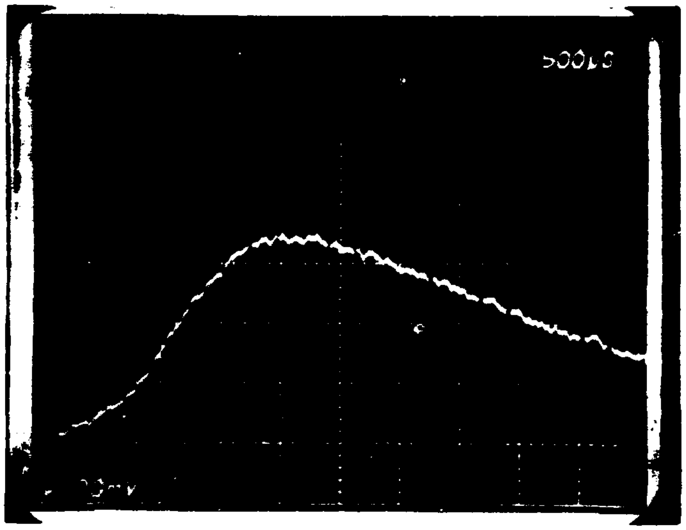

(a) Vertical: 1000 x 20 mV/div
Horizontal: 500 μsec/div

(b) Vertical: 1000 x 20 mV/div
Horizontal: 500 μsec/div

Figure 12. Diffusion signal for 2-in. galvanized steel conduit showing sense wire voltage.

were injected onto the 1 in. conduit, and the diffusion signals were measured for several values of τ with the total charge Q being held constant. Note that the charge has been injected at a time, τ, after the beginning of the pulse is, by definition,

$$Q(t) = \int_0^t Ic(t)\, dt. \qquad \text{[Eq 14]}$$

For an RC discharge of the type used in this experiment

$$Q(t) = \int_0^t \frac{V}{R} e^{\frac{-t}{RL}} dt \qquad \text{[Eq 15]}$$

so that

$$Q(t) = VC\ [1 - e^{\frac{-t}{RL}}]. \qquad \text{[Eq 16]}$$

Hence, as $t \to \infty$

$$Q = CV \qquad \text{[Eq 17]}$$

which is constant for these pulses. The results are given in Figure 13.

It is apparent from the pictures in Figure 13 that neither the pulse shape nor the peak-current magnitude affected the response shape or magnitude for impulses, which is as expected since Q remained constant, and the pulses were of sufficiently short duration. The diffusion signal for the 1-in. galvanized-steel conduit remains the same until the time constant of the current, τ, is increased to about 20 µsec at which time there is a perceptible change in the diffusion signal.

Conclusions. From the results presented in the previous section, the function for $v_I^n(t)$ and the value of M can be obtained by normalizing the data given in Figures 11 and 12. The values for $v_I^{*n}(t)$ can be obtained for 1-in. and 2-in. galvanized-steel conduit. These functions agree with the analytical value for $v_I^{*n}(t)$. From values given in Table 1 the value for M can be found. Using Eq 1-12, the sense-wire diffusion current for any conduit-current sense-wire connection and conduit length can be found. This provides a base-line signal for the conduit system and should give a meaningful basis for use in evaluating the seriousness of the leakage signals described in the next two chapters.

4 CONDUIT LEAKAGE SIGNALS DUE TO POOR COUPLING ASSEMBLY

Introduction. The diffusion signal described in Chapter 3 provides a minimum signal level that will always occur on conductors inside an excited conduit. In addition, a considerably larger signal can also be

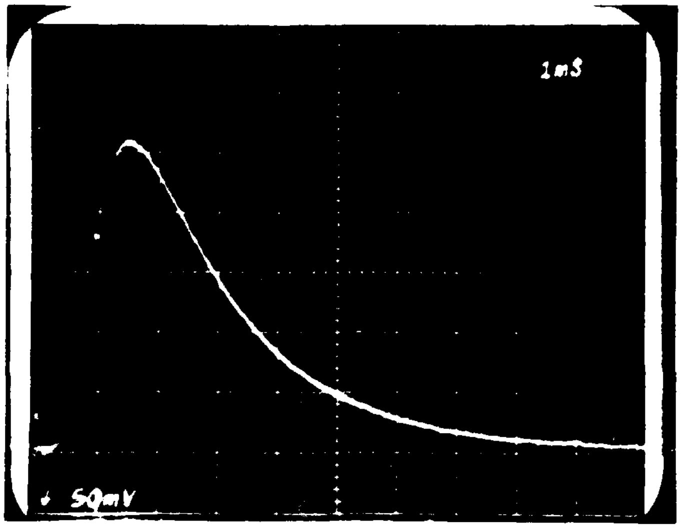

(a) Response of conduit to current pulse:

$I(t) \approx 200\, e^{\frac{-t}{30\mu sec}}$ amps (Q = CV = 6.0 x 10^{-4} coulomb).

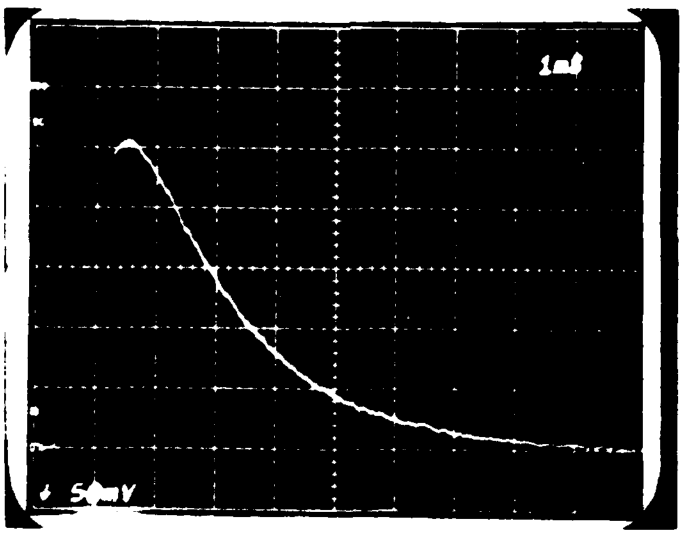

(b) Response of conduit to current pulse:

$I(t) \approx 60 e^{\frac{-t}{10\mu sec}}$ amps (Q = CV = 6.0 x 10^{-4}

Figure 13. Demonstration of impulse response (response of 1-in. galvanized steel conduit).

present, due to leakage of the external fields through holes or flaws in the conduit system. These leakage signals are mainly due to imperfections in the conduit runs. A possibility for a leak exists any place where there is a break in the metal continuity, such as where conduit sections are joined or where hardware items are connected to conduit sections. These leaks are usually due to poor assembly, such as improperly-tightened couplings or rusted threads, or improper design of conduit hardware such as some pull box covers, flexible conduits, or unions.

The leakage due to conduit hardware varies from item to item and is generally due to inadequate design. This problem is discussed in detail in Chapter 5. The leakage at points where couplings are installed between conduit sections and between conduits and conduit hardware is almost always a case of poor assembly (improperly tightened threads). This is a general problem not related to specific conduit items and is discussed next.

Background. The conduit runs utilize standard 10-ft sections of conduit, which are threaded on each end with standard pipe thread and then joined with taper-threaded couplings. Items of conduit hardware, such as unions, condulets, and flexible conduits, have either male- or female-threaded ends to which the conduits can be either directly coupled or coupled through threaded couplings. Conduits are coupled to pull boxes or junction boxes by female-threaded hubs.

At the SAFEGUARD site the specified procedure for assembling conduit runs requires that the conduit threads be brushed clean with a wire brush and that a coating of conductive compound be applied before joining the conduit sections. The joint should then be assembled and securely tightened with a pipe wrench. According to CERL tests described later in this report, when this procedure is followed the shielding at the joint is as good as the conduit itself.

Unfortunately, there were indications that the assembly procedures described in the preceding paragraph were not completely followed. Some of the conditions that might exist include corrosion of the conduit threads (especially when the conduit has been threaded in the field, thereby removing the galvanized coating), improper tightening of the conduit couplings, and improper application of conductive compound.

Since insufficient information was available regarding the degradation caused by these coupling conditions, a study was performed to evaluate improper assembly conditions.

Experimental Procedure. The EMP evaluation of conduit-coupling conditions

(for threaded joints) was made with tapered-threaded couplings* because they were the only conduit hardware with which thread-mating location was the only possible leakage point. The results, however, should be applicable to any piece of conduit hardware that threads into a conduit run and has threading similar to the couplings.

The test setup is essentially as described in Chapter 2. Test conduits were assembled under various controlled coupling-assembly conditions. These conduits were then used as the ground side of the transmission line, and measurements were taken on the sense wire inside the test sample. The sense-wire measurement included open-circuit voltage, short-circuit current, and the voltage and current across a 100 Ω sense-wire termination resistor.

Because of the low level of current for many of the test samples, the Adelco probe and Avantek amplifier described in Chapter 2 were used. For the higher level signals, the Adelco current probe and balun combination (with 50-ohm termination) were used to measure the sense-wire current. Even with the conduit samples with relatively low leakages, some amplification of the Adelco probe signal was necessary. For intermediate level signals, the amplification of the Avantek wide-band amplifier was sufficient. For extremely weak signals, the Avantek amplifier and the Channel 1 oscilloscope preamplifiers were cascaded. The Channel 1 preamplifier provided an additional gain of 14 dB (5 numeric). Using the maximum gain instrumentation configuration, the minimum measurable sense-wire current was 3.5 μA.

In measuring sense wire voltages, direct signal measurements were made with a Tektronix P-6006 probe. This probe has 20 dB of attenuation, but a low capacitance (7 pF) that permits fast rise-time measurements. The minimum open-circuit voltage measured during the tests (including the solid conduit reference) was never less than 10 mV peak to peak. This is apparently due to a combination of the limit of the shielding effectiveness of the entire test assembly and the cavity resonance of the shielded enclosure. The P-6006 probe with cascaded oscilloscope amplifiers was capable of displaying the minimum signal; and, hence, it was unnecessary to use a probe of lower attenuation. Experimentation with a Tektronix P-6046 differential FET probe showed that no advantage was gained by use of the balanced differential probe.

The transmission line was terminated in its characteristic impedance of 200 Ω, and the pulser was set to fire at 30 kV. Thus, the conduit current had a 150-amp peak, 3-nsec rise time, and 4-μsec (e-fold) fall time and is shown in Figure 2.

* The couplings used at the SAFEGUARD site were to be taper-tapped rather than the normally supplied straight-threaded couplings. The couplings tested were identical to those used at the SAFEGUARD site.

Prior to beginning the test phase of this investigation, a study was made to evaluate the test facility for leakage signals and noise. This evaluation was accomplished by replacing the te'rt conduit sample with a solid conduit and then making the sense-wire measurements. Using the test setup described earlier, there was no detectable leakage signal (Figure 14(a)) during the time period of interest (0 to 250 nsec). Some diffusion current (Figure 14(b)) was detected at times greater than 205 nsec, but the frequency response of the instrumentation was inadequate to accurately measure this signal (the diffusion signal described in Chapter 3).*

Test Samples. The test samples were made from standard 10-ft sections of galvanized rigid-wall steel conduit. The 10-ft sections were cut in half and the cut ends were threaded. In this way, both factory-cut threads and field-cut threads were available for testing. After the two sample halves were cut and threaded, they were assembled into a 10-ft test sample by using a taper-threaded coupling obtained from the SAFEGUARD site. After assembly of the test sample, the end threads were cleaned with a power wire brush and coated with Chomerics 4331 conductive compound. The end cap shown in Figure 4 with the sense wire attached was wrench-tightened onto one end of the test sample. The other end of the test sample was wrench-tightened onto the conduit stub in the shielded chamber with the sense wire protruding into the chamber. After installing the test sample, the remainder of the transmission line was assembled, the pulser was connected, and the sample was tested.

Forty-two conduit conditions were tested. These conditions included:

a. Different types of conductive compound.

b. Different levels of hand-tightness vs wrench-tightness used in coupling assembly.

c. Clean threads and couplings vs rusted threads and couplings vs rusted and aged threads and couplings.

d. Properly thinned compounds vs overly thinned compounds.

e. Different methods of compound application.

The 42 conditions that were tested are listed in Table 2 and include the above comparisons a. through e. in a variety of combinations.

* The limited low-frequency response of the Adelco probe shows the diffusion current as a damped sine wave rather than as the pulse shown in Chapter 3. The pulse of Chapter 3 was measured by a technique that provided response to 0 Hz frequency.

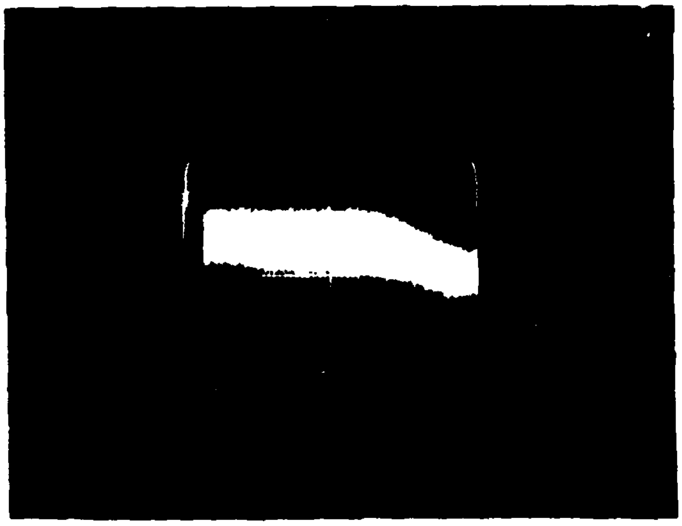

(a) Solid conduit showing start of diffusion current (vertical scale, 7.3 μA/div; horizontal scale, 50 μsec/div).

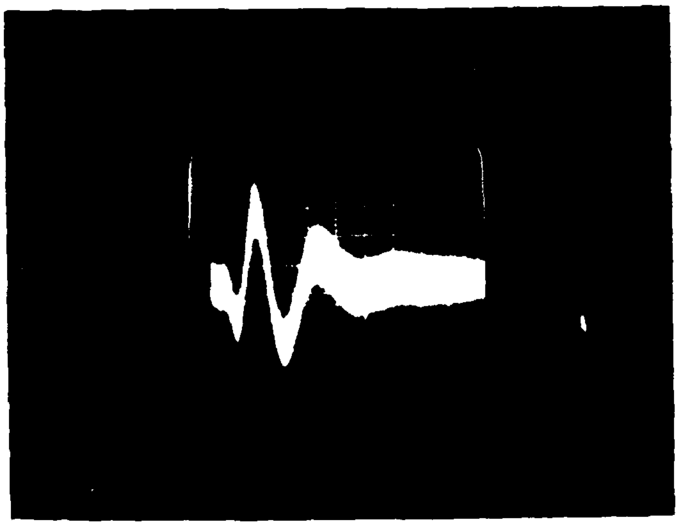

(b) Diffusion current (vertical scale, 7.3 μA/div; horizontal scale, 500 μsec/div).

Figure 14. Sense-wire short-circuit current.

Table 2

Test Samples of 1-In. Conduit

Coupling Descriptions	Sample Numbers		
	Galvanized Factory-Cut Threads	Rusted Threads	Rusted and Aged Threads*
HT Plain	1	15	15
WT Plain	2	16	16
HT BA CC1	3	17	17
WT BA CC1	4	18	18
HT SA CC1	5	19	19
WT SA CC1	6	20	20
HT FAJ CC1	7	21	21
WT FAJ CC1	8	22	22
HT TSA CC1	9	23	23
WT TSA CC1	10	24	24
HT FAJ CC2	11	25	25
WT FAJ CC2	12	26	26
HT FAJ CC3	13	27	27
WT FAJ CC3	14	28	28

HT = hand-tight
WT = wrench-tight
BA = external bead
SA = stick-applied
FAJ = factory-approved joint, compound brushed in prior to assembly
TSA = thinned, stick-applied
CC1 = Chomerics 4331
CC2 = Eccoshield VX
CC3 = Chomerics 4066

* = samples 15-28 were tested twice: once assembled with rusted threads and before aging, and again after aging

The types of compounds compared included Chomerics 4331, Chomerics 4066, and Eccoshield VX. The methods of application include brush-applied (the compound is brushed into the threads), stick-applied (the compound is simply dabbed onto the threads), and bead-applied (the compound is applied as a bead around the edge of the coupling after assembly, with no compound applied to the threads prior to assembly). Unless otherwise specified, the compounds were used at the manufacturer's approved consistency. The one thinned-compound test used Chomerics 4331 compound thinned with 3 parts N-heptane by volume.

The types of thread conditions tested included no corrosion, threads corroded prior to assembly, and threads corroded prior to and after assembly. The latter is called a rusted and aged sample and was made by taking the rusted samples after they had been tested, subjecting them to additional corrosion, and then retesting. The method of corroding and aging the test samples is described in detail in the following section.

In assembling the test samples, three levels of hand tightness (2.5 ft-lb, 5 ft-lb, and 10 ft-lb) were used in addition to the wrench-tightened joint (200 ft-lb). Ten ft-lb was the CERL measured value for the maximum torque the "average man" can apply to a 1-in. conduit by hand. Two hundred ft-lb was the maximum torque that could be applied without deforming the conduit.

One sample was used for all three levels of hand-tightness. After measurements were made at 2.5 ft-lb, the sample was tightened to 5 ft-lb and retested, and then tightened to 10 ft-lb and retested. For the rusted samples, a second sample was used for the wrench-tight case. In this way, handtight and wrench-tight rusted samples were available for aging. Thus, there were no 2.5 ft-lb or 5 ft-lb rusted and aged samples.

Rusting and Aging of Conduit Samples. In order to conduct the conduit tests on corroded and aged conduit joints, it was necessary to produce accelerated corrosion on the threads and couplings of the test conduit. This was accomplished by use of a specially constructed environmental chamber in which the conduit sample could be exposed to an atmosphere of elevated temperature and high relative humidity. The construction and operating characteristics of this environmental chamber and the method of corroding the test samples are described next.

The environmental chambers available at CERL were not large enough to handle the assembled 10-ft test samples that were used in this test program. Therefore, a chamber was constructed specifically for this purpose. The chamber is shown in Figure 15 and consists of a 16-ft long section of a 24- by 12-in. heating duct into which 25 test samples can be placed on wooden-holding racks. The ends of the duct were fitted with doors and air was forced through the duct by small fans located at either end. An air-return path was provided by a 6-in. diameter circular duct. The air was heated by a thermostatically controlled heating

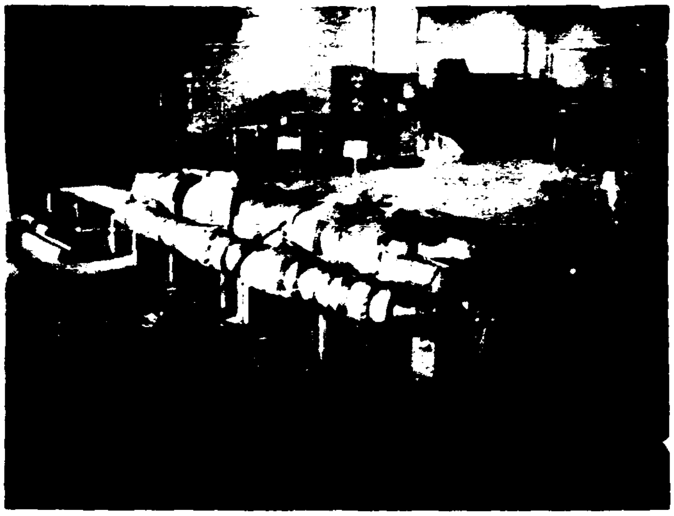

Figure 15. Environmental chamber for rusting and aging conduit samples.

element located in the fan case at one end of the chamber. The air was saturated with water vapor by means of a vaporizer placed in a water reservoir at the same end of the chamber as the heating element. The entire chamber was covered with a 4-in. layer of fiberglas insulation to minimize heat loss and temperature gradients. In order to monitor temperature and humidity, wet and dry bulb temperatures were measured with thermocouples placed in the center of the chamber. Both temperature readings were recorded on a chart recorder.

Ideally, this chamber should be capable of holding specified dry- and wet-bulb temperatures constant over an extended period of time. Practically, however, heat loss from the chamber combined with the thermal inertia of the chamber and thermostat cause these values to vary with time. These variations tended to occur on a 1 3/4-hr cycle. The heater operated at approximately 140°F with the wet- and dry-bulb temperatures indicating 100 percent relative humidity. It remained on for approximately 20 min, driving the dry-bulb temperature up to 185°F. This increase in dry-bulb temperature caused a decrease in the relative humidity, with the moisture content of the air remaining approximately fixed, and the wet-bulb temperature rising only 5°F. When the heater shut off, the dry-bulb temperature fell rapidly (approximately 2 min) to 155°F with a slight increase in wet-bulb temperature. This was followed by a slow decrease in both temperatures during the following 1 hr and 25 min before the heater turned on again. Over the 1 3/4-hr cycle, the average dry-bulb temperature was approximately 150°F--with a moisture content of approximately 0.15 lb of water vapor per lb of dry air.

The 10-ft conduit samples were cut into two equal pieces and the cut ends threaded to standard pipe-thread specifications. After cutting

the threads, they were cleaned with a solvent to remove any coating of grease and thread-cutting oil that would retard the rusting process. The threading of the conduit removed the galvanizing from the pipe and allowed rust to form on the exposed threads. After the test threads were prepared, the samples were placed in the corrosion chamber under the atmospheric conditions described above.

After the first day in the chamber, rust started to form on the threads of the samples; the amount of rust, however, varied greatly from sample to sample and even varied considerably on an individual sample. Subsequent corrosion slowed down considerably so that after 3 wk in the chamber, only a few conduit samples had uniform corrosion. The majority of the samples had areas that were completely free of corrosion. Because of the limited time available in the test, it was necessary to accelerate the corrosion process. A dilute salt-water solution (approximately 1/3 cc of salt in 6 oz of water) was prepared and painted onto the threads of half the test samples. After 1 more day in the chamber, it was visually determined that the salt-treated samples were uniformly coated with a heavy layer of rust. These samples were then removed from the chamber and the remaining samples were treated with the salt solution and put back into the chamber for an additional day of corrosion. These samples were then used to make up the test samples described earlier.

In order to compare the results of these tests with other test results and also to compare the test rust conditions with those found in the field, a method of quantitatively measuring the rust layer was needed. The method used was to cut the threads from a typical test sample and take four slices of thread (along the long axis of the conduit) at 90° increments around the edge of the conduit. These samples were then examined under a microscope to determine the thickness of the rust layer. Results showed that the rust layer had an average thickness of approximately 140 μm. The thickness of the rust layer, however, varied greatly from the tip of an individual thread to its base---with approximate thickness at the base, 225 μm, and at the tip, 75 μm. In addition, there was a factor of 2 variation in the rust thickness between the four slices taken around the edge of the conduit. This type of measurement apparently provides the best means of comparing different rust samples, especially since the rust conditions in the field are unknown.

After testing the rusted conduit joints described above, the assembled samples were subjected to additional accelerated rusting in order to simulate aging of buried conduit joints. The accelerated aging was conducted in the environmental chamber described earlier, but the heating element was not used. The air was heated solely by the steam emitted from the vaporizer. Using this method, the chamber temperature remained relatively constant at 115°F. In addition, the relative humidity was kept constant at near 100 percent. The net effect of using this method was a lowering of the chamber temperature by 35°F in return for a stable temperature and higher relative humidity. The moisture content of the

air using this method was about 0.07 lb of water vapor per lb of dry air.

After several days of exposure to the above environmental conditions, visual inspection of the samples indicated that considerable additional corrosion was present. It could be observed through the conductive compound that covered the threads of some of the samples. This corrosion was definitely occurring more rapidly than that on the original bare threads, and therefore, these samples were left in the chamber for aging only 10 days.

Since the measurement of the thickness of rust by means of a microscope is a destructive test, it was not possible to determine the rust thickness after aging. Therefore, a visual inspection was used to determine the condition of the conduit joint following the aging process.

Test Results. Data presented in this section result from the conduit tests described earlier. Table 3 (placed at the end of this chapter) is a summary of these data, and was obtained from the oscilloscope pictures taken as described in the earlier section on Experimental Procedure. A typical set of these oscilloscope pictures is presented in Figure 16. The wave forms shown in this figure are nearly identical for all the samples, with the exception of magnitudes; thus, only this one typical set of pictures is presented. However, CERL is filing all of the oscilloscope pictures taken during the study. The pictures taken for each sample include:

a. The conduit current, monitored for each test and kept constant at 150 amp to allow direct comparison of data for different test samples (Figure 2).

b. The sense-wire, short-circuit current using a time base which shows the current wave-form rise time (Figure 16 (a)).

c. The sense-wire, short-circuit current using a time base which shows the current wave-form fall time (Figure 16(b)).

d. The sense-wire current with a 100-ohm termination with a time base which shows the complete wave form (Figure 16(c)).

e. The sense-wire current with a 100-ohm termination with a time base which shows the current wave-form rise time (Figure 16(d)).

f. The voltage across the 100-ohm resistor showing the complete wave form (Figure 16(e)).

g. The sense-wire, open-circuit voltage on a time base showing the initial oscillatory portion of the wave form (Figure 16(f)).

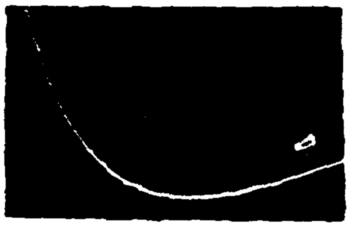

(a) Short-circuit current; vertical scale, 51.4 mA/div; horizontal scale, 0.5 μsec/div (sample #27, 2.5 ft-lb).

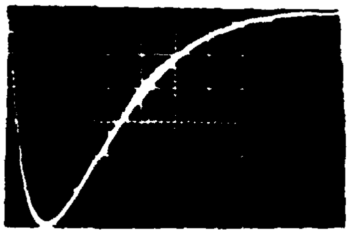

(b) Short-circuit current; vertical scale, 25.7 mA/div; horizontal scale, 2 μsec/div (sample #27, 5 ft lb).

(c) Sense-wire current with 100 ohm termination; vertical scale, 2.57 mA/div; horizontal scale, 1 μsec/div (sample #27, 2.5 ft-lb).

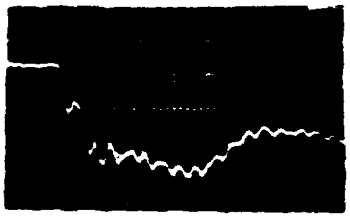

(d) Sense-wire current with 100 ohm termination; vertical scale, 2.57 mA/div; horizontal, 20 nsec/div (sample #27, 2.5 ft-lb).

(e) 100-ohm termination voltage; vertical scale, 200 mV/div; horizontal scale, 1 μsec/div (sample #27, 2.5 ft lb).

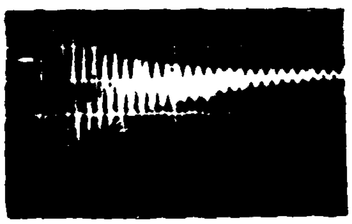

(f) Open-circuit voltage; vertical scale, 500 mV/div; horizontal scale, 0.2 μsec/div (sample #27, 2.5 ft-lb).

Figure 16. Typical set of oscilloscope pictures.

The data taken from the oscilloscope pictures, and listed in Table 3, include peak values of sense-wire, short-circuit current, peak values of the voltage across a 100-ohm termination, the current through a 100-ohm termination; peak-to-peak values of the open-circuit voltage; and the rise and fall times for the short-circuit current. The rise time measured was the time required for the wave form to reach 90 percent of its peak value. The fall time (e-fold) was the time measured from peak to 37 percent of peak (i.e., 1/e time constant).

Table 3 also includes the sample number from Table 2 and a description of the sample, and indicates which samples have been used in multiple tests. For example, sample 1c was a hand-tight sample with no compound and sample 3b was the same sample with an external bead applied. In addition, where several samples of the same type were tested to obtain an indication of statistical variation, each sample is distinguished by a letter following the sample number.

Conclusions. Data applied to any application other than those similarly derived (as discussed in this chapter) must be carefully interpreted. This is important because the current on the conduit flows over the coupling, and if any holes or flaws exist at the coupling, fields will be induced inside the conduit at that point. These fields then excite the transmission line made up of the conduit and sense wire and produce a sense-wire signal. It is this signal that is actually being measured. Therefore, the configuration of the sense-wire transmission line will have a great effect on the measured signal.

Early measurements were made with the sense wire terminated in an impedance near the characteristic impedance of the sense-wire conduit transmission line (approximately 110 ohms). This measurement minimizes the effects of the sense-wire circuit on the sense-wire signal, in that the signal on a matched, terminated sense wire will have no reflections and be an accurate representation of the leakage signal. Unfortunately, the sense wire does not form a uniform transmission line. Thus, the characteristic impedance varied along the line. In addition, when the sense wire was terminated with a load in the range of its characteristic impedance, the signal levels were extremely low and the leakage signal for many of the conduit conditions could not be measured. When a shorted sense wire was used, the reflections from the shortened terminations caused a build-up of the sense-wire signal and an effective increase in the measurement sensitivity. Because of this build-up effect, the magnitude of the sense-wire signal is dependent on the length of the conduit sample, since this determines the time between reflections.

The shorted sense wire also greatly affects the rise time of the induced signal. The rise times reported are more a function of the sense-wire circuit than the coupling condition. Although absolute values for leakage due to coupling conditions are not reported, the data can be used to provide comparison between variations in coupling conditions--which is the basic intent of this study.

An additional consideration in analyzing the results presented herein is that the fall times will be partially determined by the limited low-frequency response of the Adelco probe, as discussed in the section on Experimental Procedure.

Additional coupling studies using differential-mode sense wires--that is, sense wires not connected to the conduit itself, are reported in the next chapter. CERL currently has a study underway to determine absolute values for coupling leakage and to develop a methodology for predicting sense-wire signals using these absolute leakage data. This study will concentrate on one or two coupling conditions since the relative variations between coupling conditions can be found herein.

The results of this report should not be used to determine whether different coupling conditions are acceptable, since this is highly dependent on types of cables inside the conduits, susceptibility of the equipment to which these cables are connected, length of the conduit runs, cable terminations, and number of defects found in any given conduit system.

However, some general conclusions or guidelines can be drawn. First, tightness of the joint appears to be the most important factor in determining the amount of leakage that will occur at a coupling. The condition of the threads also has a significant effect, but not nearly as much as the tightness of the coupling. Finally, the use of any of the compounds tested seems to have only a minor effect on the leakage at a given defect.

Table 3

Conduit Test Data*

Test Sample			Short-Circuit Current			$V_{Open\ Ckt}$	V_{100}	I_{100}
No.	Description	Torque Ft - lb	Peak (mA)	Rise Time (μsec)	Fall Time (μsec)	P-P (mV)	Peak (mV)	Peak (mA)
1a	Clean FGT, HT No Compound	2.5	18.0	1.1	5.2	350	120	7.7
		5.0	13.9	0.9	4.6	430	115	1.7
		10	19.0	0.8	4.4	340	130	1.7
1b	Clean FGT, HT No Compound	2.5	3.9	1.0	4.1	NT	NT	NT
		10	1.3	1.1	5.0	28	21	0.08
1c**	Clean FGT, HT No Compound	10	3.95	1.1	4.4	94	NT	NT
1d	Clean FGT, HT No Compound	2.5	29.8	0.65	4.4	1080	330	3.21
		5.0	7.57	1.0	5.6	150	62	0.57
		10	1.6	1.5	7.0	26	17	0.054

*See notes at end of table.
**Same sample as No. 3b.

Table 3 (cont'd)

Test Sample			Short-Circuit Current			$V_{Open\ Ckt}$	V_{100}	I_{100}
No.	Description	Torque Ft - lb	Peak (mA)	Rise Time (μsec)	Fall Time (μsec)	P-P (mV)	Peak (mV)	Peak (mA)
2a	Clean FGT, WT No Compound	200	0.014	9	15	--	--	--
2b	Clean FGT, WT No Compound	200	0.003	--	--	--	--	--
2c	Clean FGT, WT No Compound	200	0.007	--	--	--	--	--
2d	Clean FGT, WT No Compound	200	0.005	--	--	--	--	--
3a	Clean FGT, HT Chomerics 4331 External Bead	10	5.3	1.5	6.0	84	24	.29
3b*	Clean FGT, HT Chomerics 4331 External Bead	10	3.42	1.0	4.5	94	NT	NT
4a	Clean FGT, WT Chomerics 4331 External Bead	200	0.003	--	--	36	--	--

*Same sample as No. 1c.

Table 3 (cont'd)

Test Sample			Short-Circuit Current			$V_{Open\ Ckt}$	V_{100}	I_{100}
No.	Description	Torque Ft - lb	Peak (mA)	Rise Time (μsec)	Fall Time (μsec)	P-P (mV)	Peak (mV)	Peak (mA)
4b	Clean FGT, WT Chomerics 4331 External Bead	200	0.005	--	--	22	--	--
5	Clean FGT, HT Chomerics 4331 Stick Applied	2.5	19.6	1.15	5.2	380	125	1.53
		5.0	8.1	1.35	5.4	110	39	0.44
		10	0.38	1.8	6.8	20	15	0.022
6	Clean FGT, WT Chomerics 4331 Stick Applied	200	0.003	--	--	--	--	--
7a	Clean FGT, HT Chomerics 4331 Brush Applied	2.5	2.5	1.9	6.4	17	14	0.09
		5.0	4.9	1.4	6.0	44	31	0.35
		10	0.63	2.0	7.6	19	17	--
7b	Clean FGT, HT Chomerics 4331 Brush Applied	2.5	8.0	1.0	5.8	95	42	0.40
		5.0	4.7	1.5	6.0	34	16	0.145
		10	0.7	2.3	7.4	19	13	--

Table 3 (cont'd)

Test Sample			Short-Circuit Current			$V_{Open\ Ckt}$	V_{100}	I_{100}
No.	Description	Torque Ft - lb	Peak (mA)	Rise Time (μsec)	Fall Time (μsec)	P-P (mV)	Peak (mV)	Peak (mA)
7c	Clean FGT, HT Chomerics 4331 Brush Applied	2.5	14.1	1.3	5.8	275	NT	NT
		5.0	6.7	1.5	5.8	80	NT	NT
		10	0.5	1.9	7.2	NT	NT	NT
8a	Clean FGT, WT Chomerics 4331 Brush Applied	200	0.040	10	20	--	--	--
8b	Clean FGT, WT Chomerics 4331 Brush Applied	200	0.003	10	20	--	--	--
9	Clean FGT, HT Chomerics 4331, Thinned Stick Applied	2.5	13.6	0.9	4.6	420	100	2.0
		5.0	22.1	0.8	4.6	960	180	3.65
		10	2.06	1.6	8.0	27	21	51
10	Clean FGT, WT Chomerics 4331, Thinned Stick Applied	200	0.003	--	--	--	--	--

Table 3 (cont'd)

Test Sample			Short-Circuit Current			$V_{Open\ Ckt}$	V_{100}	I_{100}
No.	Description	Torque Ft - lb	Peak (mA)	Rise Time (μsec)	Fall Time (μsec)	P-P (mV)	Peak (mV)	Peak (mA)
11a	Clean FGT, HT Eccoshield VX Brush Applied	2.5	2.34	1.75	5.6	28	--	83
		5.0	3.65	1.2	4.5	90	--	212
		10	0.386	2.2	7.4	23	--	0.004
11b	Clean FGT, HT Eccoshield VX Brush Applied	2.5	1.1	1.7	7.0	22	--	0.014
		5	0.72	2.1	7.2	26	--	0.10
		10	0.008	8	30	--	--	--
12	Clean FGT, WT Eccoshield VX Brush Applied	200	0.003	--	--	--	--	--
13a	Clean FGT, HT Chomerics 4066 Brush Applied	2.5	1.75	1.32	6.05	16	16	0.060
		5	0.64	2.4	8.4	20	13	--
13b	Clean FGT, HT Chomerics 4066 Brush Applied	2.5	5.4	1.31	6.3	65	25	0.20
		5.0	0.51	1.7	8.8	20	18	--
		10	0.68	1.5	6.4	20	14	0.014

Table 3 (cont'd)

Test Sample			Short-Circuit Current			$V_{Open\ Ckt}$	V_{100}	I_{100}
No.	Description	Torque Ft - lb	Peak (mA)	Rise Time (μsec)	Fall Time (μsec)	P-P (mV)	Peak (mV)	Peak (mA)
14	Clean FGT, WT Chomerics 4066 Brush Applied	200	0.003	--	--	--	--	--
15a	Rusted, HT No Compound	2.5	205	0.84	4.4	7200	2300	26.5
		5.0	111	0.78	4.8	3000	980	6.9
		10	70	1.1	5.2	2100	480	4.1
	Sample 15a, Aged	10	216	0.98	4.8	6200	2000	22.5
15b	Rusted, HT No Compound	2.5	164	1.2	4.8	2500	620	6.2
		5.0	212	1.2	4.8	1800	NT	NT
		10	43.4	1.2	5.2	600	225	2.92
15c	Rusted, HT No Compound	2.5	6400	0.9	1*	55000	24500	257
		5.0	1030	1.3	5.0	11200	5200	57
		10	391	1.2	6.0	5400	1750	20.6

*Saturated probe.

Table 3 (cont'd)

Test Sample			Short-Circuit Current			$V_{Open\ Ckt}$	V_{100}	I_{100}
No.	Description	Torque Ft - lb	Peak (mA)	Rise Time (μsec)	Fall Time (μsec)	P-P (mV)	Peak (mV)	Peak (mA)
15d	Rusted, HT No Compound	10	340	1.1	4.8	4600	1040	16
16a	Rusted, WT	200	0.278	2.8	8	30	--	0.003
	Sample 16a, Aged	200	0.31	3.2	10	20	19	--
16b	Rusted, WT No Compound	200	0.08	3.6	9	17	--	--
16c*	Rusted, WT No Compound	200	0.233	3.8	9	26	26	--
17a	Rusted, HT Chomerics 4331 External Bead	10	700	1.75	7	4200	1500	14.9
	Sample 17a, Aged	10	1640	1.7	4.8	10100	380	39.1
17b	Rusted, HT Chomerics 4331 External Bead	10	391	1.0	4.0	5700	2200	23.6

*Same sample as No. 18b.

Table 3 (cont'd)

Test Sample			Short-Circuit Current			$V_{Open\ Ckt}$	V_{100}	I_{100}
No.	Description	Torque Ft - lb	Peak (mA)	Rise Time (μsec)	Fall Time (μsec)	P-P (mV)	Peak (mV)	Peak (mA)
18a	Rusted, WT Chomerics 4331 External Bead	200	0.292	2.7	9	16	--	--
	Sample 18a, Aged	200	0.35	2.7	9	23	21	--
18b*	Rusted, WT Chomerics 4331 External Bead	200	0.350	2.7	8	26	26	--
19	Rusted, HT Chomerics 4331 Stick Applied	2.5	1000	1.2	5.8	16000	00	61.5
		5.0	773	1.2	6	5400	2000	20.5
		10	196	1.5	6.1	1750	0	6.7
	Sample 19, Aged	10	690	1.5	7.2	8800	3800	40
20	Rusted, WT Chomerics 4331 Stick Applied	200	0.168	3.2	10	16	--	--
	Sample 20, Aged	200	0.29	3.2	7	20	17	--

*Same sample as No. 16c.

Table 3 (cont'd)

Test Sample			Short-Circuit Current			$V_{Open\ Ckt}$	V_{100}	I_{100}
No.	Description	Torque Ft - lb	Peak (mA)	Rise Time (μsec)	Fall Time (μsec)	P-P (mV)	Peak (mV)	Peak (mA)
21	Rusted, HT Chomerics 4331 Brush Applied	2.5	720	1.4	5.6	6800	2400	28.3
		5.0	440	1.3	6.4	2150	1040	11.2
		10	370	1.2	6.6	1950	920	9.0
	Sample 21, Aged	10	1030	1.5	5	3400	2250	22.1
22	Rusted, WT Chomerics 4331 Brush Applied	200	0.056	3.4	12	19	--	--
	Sample 22, Aged	200	0.024	5.5	14	14	--	--
23	Rusted, HT Chomerics 4331, Thinned Stick Applied	2.5	1100	1.4	5.7	18500	5900	66
		5.0	942	1.3	5.1	17000	5400	66
		10	1184	1.5	5.6	11200	4000	37
	Sample 23, Aged	10	3708	1.5	21.*	41000	14500	130

*Probe saturated.

Table 3 (cont'd)

Test Sample			Short-Circuit Current			$V_{Open\ Ckt}$	V_{100}	I_{100}
No.	Description	Torque Ft - lb	Peak (mA)	Rise Time (μsec)	Fall Time (μsec)	P-P (mV)	Peak (mV)	Peak (mA)
24	Rusted, WT Chomerics 4331, Thinned Stick Applied	200	0.031	7	36	21	19	--
	Sample 24, Aged	200	0.172	7.5	14	35	--	--
25	Rusted, HT Eccoshield VX Brush Applied	2.5	475	1.3	6.6	2950	1300	13.4
		5.0	566.5	1.7	6.8	2200	1028	10.3
		10	360	1.8	6.8	2300	1000	9.8
	Sample 25, Aged	10	474	1.65	6.0	3400	1300	12.3
26	Rusted, WT Eccoshield VX Brush Applied	200	1.7	1.8	6.8	16	--	--
	Sample 26, Aged	200	0.68	3.2	9.0	22	--	--
27	Rusted, HT Chomerics 4066 Brush Applied	2.5	283	1.4	7	2300	840	8.2

Table 3 (cont'd)

Test Sample			Short-Circuit Current			$V_{Open\ Ckt}$	V_{100}	I_{100}
No.	Description	Torque Ft - lb	Peak (mA)	Rise Time (μsec)	Fall Time (μsec)	P-P (mV)	Peak (mV)	Peak (mA)
27	Rusted, HT Chomerics 4066 Brush Applied	5.0	144	1.2	6	1800	620	5.9
		10	111	1.3	5.5	760	320	3.7
	Sample 27, Aged	10	730	1.4	5.5	5200	2200	22.6
28	Rusted, WT Chomerics 4066 Brush Applied	200	0.47	2.8	9.0	14	--	--
	Sample 28, Aged	200	0.124	4.3	11	28	--	--
--	Clean FGT Open Coupling Strap Jumper	0	1030	0.6	1.9	2300	NT	NT
--	Rusted Open Coupling Touching but Not Threaded	0	2200	0.4	4.4	25000	10000	NT

Notes:
1. Each data block is one sample unless otherwise noted. 2. FGT = factory galvanized thread. 3. HT = hand-tight; WT = wrench-tight. 4. NT = data not taken for that sample. 5. A dash (-) indicates a signal too small to measure. 6. Rise time was measured from 0 to 90 percent of peak. 7. Fall time was measured from peak to 37 percent of peak.

5 CONDUIT LEAKAGE CURRENT FROM CONDUIT RELATED HARDWARE

Introduction. Chapter 4 examined the problems of electromagnetic leakage into a conduit system due to improper assembly of the conduit runs. It was shown that proper assembly of conduit runs would create a conduit system with good EMP shielding. Unfortunately, even when these systems are assembled correctly, leakage of external radiation into the conduit can exist due to flaws or defects in the design or construction of the conduit hardware. This usually occurs because these items are often conventional hardware items and are not designed with consideration of EMP shielding. Thus, mating surfaces, such as in conduit unions and around covers of junction boxes, often do not form good EMP shields. With some items, such as some flexible conduits, the design may rely on materials of insufficient thickness to provide adequate shielding for diffusion currents. In either case, the use of conduit hardware items will generally create a degradation in the shielding of the conduit runs. This part of the study was conducted to investigate these additional hardware items, to evaluate their shielding characteristics, and to compare their shielding properties to the various coupling conditions discussed in Chapter 4.

In addition to hardware studies, this chapter examines the problems caused by the heating of couplings due to welding in the vicinity of the coupling. Also discussed are the repeatability of the data in this report, the comparison of lab-rusted items with field-rusted items, and the effect of sense-wire configuration on reported data.

In all tests reported in this chapter, the short-circuit current was the measurement of interest since it was the most accurate and would most readily allow for comparison with the diffusion and coupling-current data of the previous chapters.

Experimental Procedure. The test setup was as described in Chapter 2. Test conduits were assembled containing the hardware item or test condition to be evaluated. These test conduits were then used as the ground side of the transmission line and short-circuit current measurements were made on the sense wire inside the test conduit. Unless otherwise stated, the pulser was adjusted to inject the 150-amp peak current pulse of Figure 2 onto the transmission line.

Because the short-circuit, sense-wire current signals in these tests were considerably larger than those associated with the coupling study, the Tektronix P6021 current probe could be used. As described in Chapter 2, this probe was chosen for its good low-frequency response, which provided an accurate measure of the short-circuit current fall times. Where voltage measurements were taken, a Tektronix P6053A voltage probe was used.

Test Sample Preparation

Explosion Proof Unions. Two 5-ft sections of the appropriate size of rigid-wall steel conduit were joined together using samples of 1-in. UNF, 1-in. UNY, and 4-in. UNF explosion-proof unions (Figure 17). Each resulting test sample was approximately 10 ft long. One additional test sample was prepared using a standard 1-in. UNF union that had been modified to have flat-mating surfaces similar to 2 in. and larger UNF unions, rather than the ribbed-mating surfaces that are standard on 1-in. UNF unions. The criteria for this modification were obtained by measuring both the flatness and finish of the mating surfaces of a standard 2-in. UNF union. Both halves of the 1-in. union were machined and ground to provide a surface with the same finish as the 2-in union (Figure 18).

Each test sample, in turn, was inserted into the conduit serving as the ground side of the transmission line (Figure 19). The relationship between the tightness and the EMP-shielding effectiveness of each union was investigated by taking measurements at various levels of tightness (as measured in ft-lb of torque applied). In addition, some samples had a coating of conductive compound* applied to the conduit and union threads prior to assembly. Some samples also had a coating of conductive compound applied to the union-mating surfaces prior to assembly and test. Table 4 summarizes the various combinations tested.

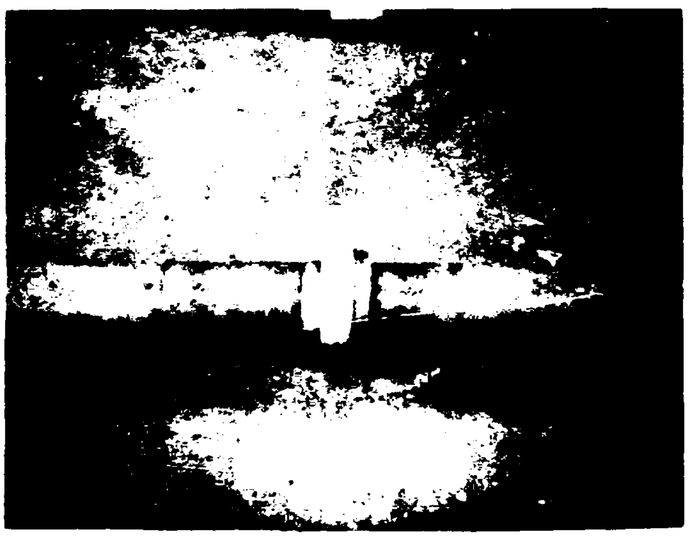

Figure 17. Test sample of 4-in. explosion-proof union installed on conduit sections.

* Chomerics 4331 conductive compound, distributed by Chomerics, Inc., Arlington, MA.

Figure 18. Standard 2-in. and modified 1-in. UNF unions showing flat-mating surfaces.

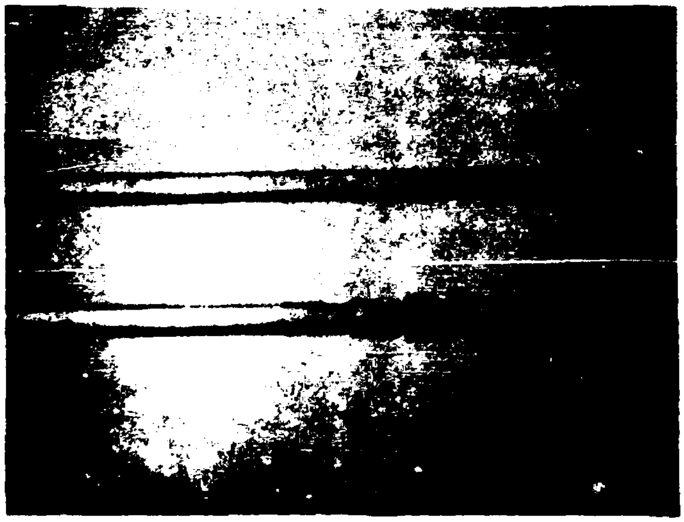

Figure 19. One-in. explosion-proof union (UNY) installed in transmission line.

Table 4

Summary of Explosion-Proof Union Test Combinations

DESCRIPTION	TEST CONDITION
1-in. Male-Female UNY (standard) without compound	(1) Hand-tight (10 ft-lb) (2) Wrench-tight (150 ft-lb)
1-in. Female-Female UNF (standard) without compound	(1) Hand-tight (10 ft-lb) (2) Wrench-tight (150 ft-lb)
1-in. Female-Female UNF (modified)	(1) Hand-tight (10 ft-lb) (2) Hand-tight (10 ft-lb) with Chomerics 4331 compound on mating surfaces (3) Wrench-tight (150 ft-lb) with Chomerics 4331 compound on mating surfaces
4-in. Appleton UNF Union without compound	(1) Hand-tight (2) Wrench-tight (1200 ft-lb)

Four-In. Conduit Couplings. The 4-in. conduit-coupling samples were tested in much the same way as were the 1-in. conduit couplings (Chapter 3). The 4-in. conduit-coupling data reported herein can be compared to the earlier 1-in. conduit-coupling data, and provide information useful for applying the 1-in. conduit test results to larger conduit systems.

Each test sample was prepared by first wrench-tightening the end cap onto a 5-ft section of 4-in. rigid-wall galvanized-steel conduit (Figure 20). A second 5-ft section was then wrenched-tightened onto the conduit stub that was attached to the shielded enclosure. The two sections were then assembled hand-tight with a coupling, and the data were taken. Additional measurements were taken after the joint had been tightened further (all four samples were tightened to 400 ft-lb of torque and two were tightened further to 1,000 ft-lb of torque). Table 5 lists the sample combinations tested. As indicated, some of the samples had clean threads and others had threads that had been allowed to rust prior to assembly. Chomerics 4331 conductive compound was applied to some of the samples. For two of the samples, the viscosity of this compound was as prepared by the manufacturer and the compound was applied using a brush. For the other sample, the conductive compound was thinned using 3 parts N-heptane to 1 part compound by volume and was dabbed onto the conduit threads using a stick.

Flexible Conduit. Samples of a number of types of flexible conduit were tested, including both Radio-Frequency Interference (RFI) tight and non-RFI tight types. Each sample was installed in the 1-in. conduit-transmission line by using sections of 1-in. conduit and reducers of the appropriate size. The length of the rigid-conduit sections was such that the overall test sample length was approximately 10 ft.

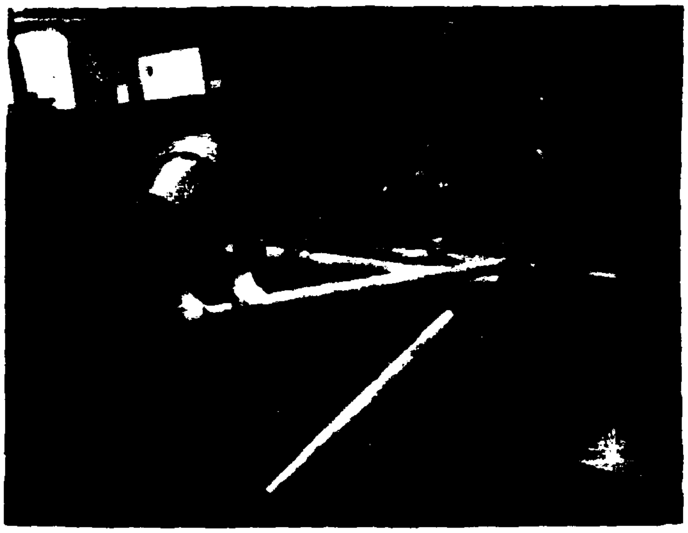

Figure 20. Four-in. conduit sample being assembled using pipe wrench and extensions.

Table 5

Summary of 4-In. Conduit Coupling Test Combinations

DESCRIPTION	TEST CONDITIONS
Non-rusted with Chomerics 4331 conductive compound	(1) Hand-tight (2) 400 ft-lb
Rusted with no compound	(1) Hand-tight (2) 400 ft-lb (3) 1000 ft-lb
Rusted with Chomerics 4331 compound	(1) Hand-tight (2) 400 ft-lb (3) 1000 ft-lb
Rusted with thinned stick applied Chomerics 4331 compound	(1) Hand-tight (2) 400 ft-lb (3) 1000 ft-lb

Two samples of non-RFI tight 1-in. flexible conduit (Sealtite)* were delivered to CERL from the SAFEGUARD site. Each sample was approximately 18 in. long when assembled with standard conduit fittings. The male threads at each end of the test sample were mated (either wrench-tight or hand-tight) with standard 1-in. taper-threaded couplings to 1-in. conduit sections (4 1/4 ft long). Each sample was tested both with and without a number-six stranded insulated-copper wire (ground wire) in parallel with the flexible section (Figures 21 and 22). Grounding lugs provided on the flexible conduit fittings were used to attach this wire.

Two samples of RFI-tight flexible conduit (bellows type produced by Anaconda Metal Hose Division, Anaconda American Brass Company, Waterbury, CT) were obtained from the SAFEGUARD site. A green polyvinyl-chloride (PVC) protective coating covered the bellows on both samples. Both samples had a 1 1/2-in. inside diameter (I.D.) and were 28 in. long. The ends of each sample were joined with a reducer to a section of 1-in. rigid-wall conduit (Figures 23 and 24). The final configuration was such that, in each case, the total length of the rigid conduit and the test sample was approximately 10 ft, with the test sample in the middle. Chomerics 4331 conductive compound (normal viscosity) was brush-applied to all threads prior to assembly, and all joints were wrench-tightened.

Additional tests were conducted using modified samples of flexible conduit procured from the manufacturer. These samples were of the same basic bellows-type design as those obtained from the site, except that the former had a special Hypermaflex (high-permeability metal) bellows** and the latter had the standard steel flexible bellows. Each had the bellows covered by one or two layers of braid sleeve (either standard galvanized steel or stainless steel). The specially procured samples had no PVC cover. Various braid-sleeve configurations were tested. Using these samples, the following tests were conducted:

a. A 1 1/2-in. I.D. conduit section with a standard steel flexible bellows and two layers of galvanized steel braid (Anaconda Part No. 2198-700, Figure 25), tested with braid intact and again with braid removed.

b. A 4-in. I.D. flexible conduit section with a standard steel flexible bellows and one layer of galvanized steel braid (Figure 26), tested (1) alone, (2) with a 1-in. wide tinned copper braid in parallel

---

* Sealtite is a brand name of Anaconda Metal Hose Division. Construction is extruded polyvinyl-chloride over a flexible spiral-linked, galvanized-steel core.

** Anaconda brand name for bellows-type flexible conduit with a core of hipernon (Westinghouse Electric Co.) or moly-permalloy (Allegheny Steel Corp.); 80 percent nickel, 20 percent iron.

Figure 21. Non-RFI tight flexible conduit sample (Sealtite) without ground wire.

Figure 22. Non-RFI tight flexible conduit sample (Sealtite) with ground wire.

Figure 23. PVC-covered 1 1/2-in. RFI tight flexible conduit sample as installed in the parallel conduit transmission line (showing reducers).

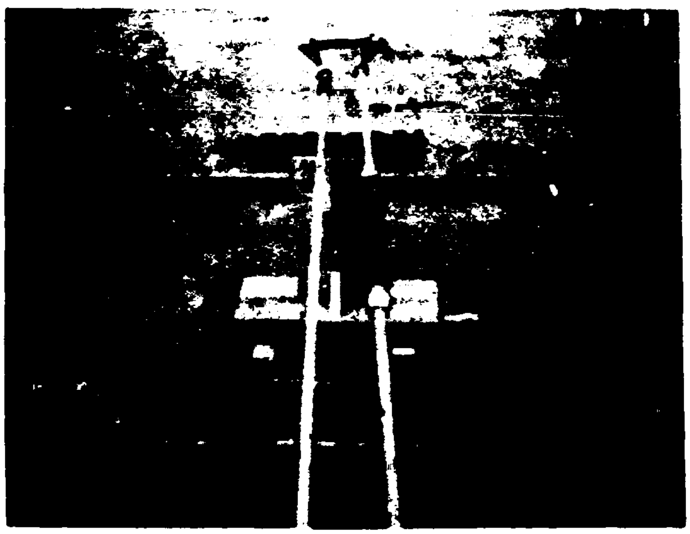

Figure 24. PVC-covered 1 1/2-in. RFI tight flexible conduit sample as installed in the parallel conduit transmission line.

Figure 25. A 1 1/2-in. flexible conduit sample with a standard steel flexible bellows and two layers of galvanized steel braid.

Figure 26. A 4-in. flexible conduit sample with a standard steel flexible bellows and one galvanized steel braid.

with the flexible section (Figure 27), (3) with a 2 1/2-in. wide tinned copper braid in parallel with the flexible section, and (4) with braid removed.

c. A 1 1/2-in. I.D. flexible conduit section with a Hypermaflex flexible bellows and one layer of stainless-steel braid (Figure 28), tested (1) with braid intact, (2) with braid disconnected from one end of the flexible section (Figure 29), and (3) with braid removed (Figure 30).

d. A 1 1/2-in. I.D. flexible conduit section with a Hypermaflex flexible bellows and two layers of galvanized steel braid (Anaconda Part No. 306971), tested with braid intact.

e. A 1 1/2-in. I.D. flexible conduit section with a Hypermaflex flexible bellows and one layer of galvanized steel braid which was secured in the normal manner at one end of the flexible section, but which was secured to the other end by an automotive screw-type clamp (to provide extension flexibility as well as lateral flexibility, Figures 31 and 32).

Except for the 4-in. flexible section which was tested in a 4-in. line, each sample was tested by inserting it in the ground leg of the parallel 1-in. conduit transmission line described earlier, using the appropriate size reducers. A 1-in. (4 in. for the 4-in. line) rigid-steel conduit was used as the other leg of the transmission line.

Condulets, Gaskets, and Covers. Several type C, cast-iron condulets, with 1-in. female threads at each end, were obtained from the SAFEGUARD site for use as test samples. Each of these condulets was supplied without a gasket, but with a cover plate stamped from approximately 1/16-in. steel. The cover was secured to the condulet by two screws, one at each end.

The condulet was mounted between two 5-ft long sections of 1-in. rigid-wall conduit (Figure 33), and the resulting assembly was used as the ground leg of the transmission line. Chomerics 4331 conductive compound (normal viscosity) was brush-applied to all threads prior to assembly, and all joints were tightened to approximately 150 ft-lb of torque.

Data were taken with the standard covers and with specially prepared 11-gauge steel covers, some of which had been flame-sprayed with tin or zinc. Tests were conducted both with and without various gasket materials. When attaching the covers with gaskets, care was exercised to prevent deformation due to excessive torque on the screws while still assuring compression of the gasket around the entire periphery. Figure 34 lists the various condulet/cover arrangements tested.

The steel-wool gaskets were made by hand-forming steel-wool pads (both coarse and fine) manufactured for general-purpose use. Each

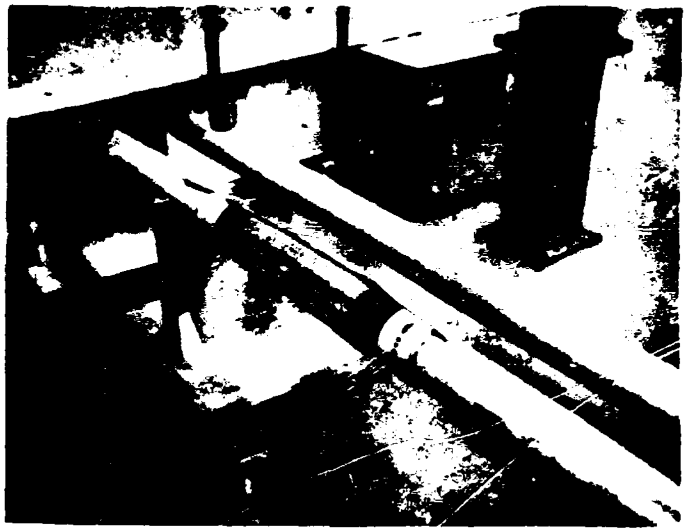

Figure 27. A 4-in. flexible conduit sample with a standard steel flexible bellows and one galvanized steel braid with a 1-in. wide tinned copper braid in parallel with the flexible section.

Figure 28. A 1 1/2-in. flexible conduit sample with a Hypermaflex flexible bellows and one stainless-steel braid with braid intact.

Figure 29. A 1 1/2-in. flexible conduit sample with Hypermaflex flexible bellows and one stainless-steel braid, showing the braid disconnected from one end.

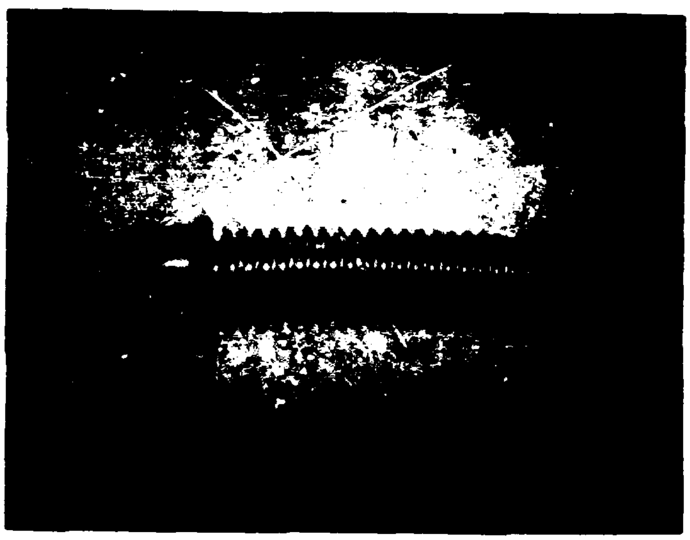

Figure 30. A 1 1/2-in. flexible conduit sample with Hypermaflex flexible bellows after the stainless-steel braid had been removed.

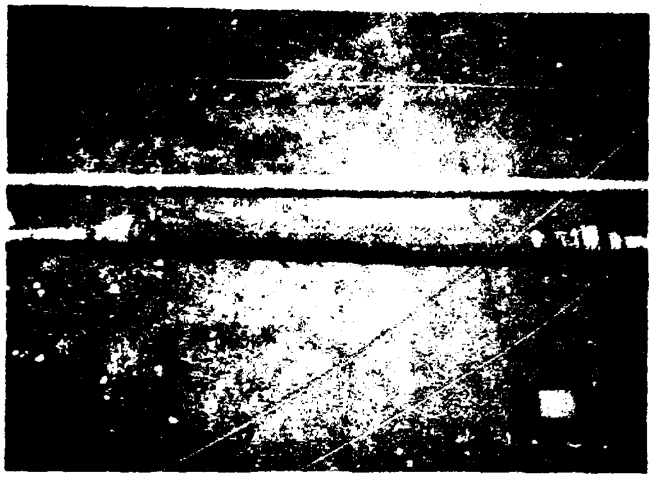

Figure 31. Specially designed 1 1/2-in. flexible conduit sample with Hypermaflex flexible bellows and one galvanized steel braid (which is normally secured to one end of the flexible section, but is secured to the other end with an automotive screw-type hose clamp).

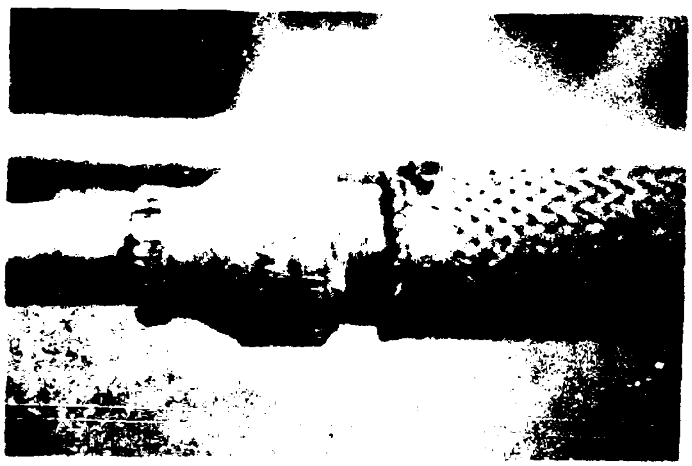

Figure 32. Specially designed 1 1/2-in. flexible conduit sample showing the automotive screw-type hose clamp used to secure one end of the galvanized steel braid.

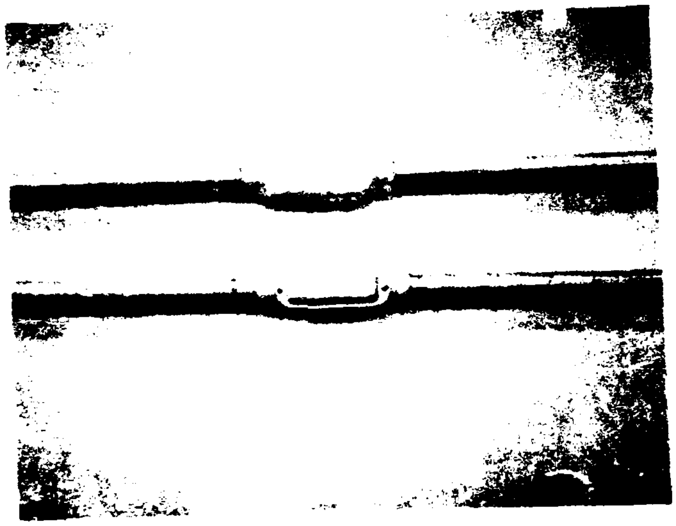

Figure 33. Condulet test samples.

1. No cover installed on condulet.

2. Condulet with standard stamped 16-gauge steel (K100) cover installed tightly using the two screws provided by the manufacturer--under the following conditions:

   a. No gasket
   b. Steel-wool gasket
   c. Chomerics 4331 gasket
   d. Tecknit-Elastomet gasket
   e. Tecknit-Elastomet gasket plus three steel shipping bands
   f. Tecknit-Elastomet gasket plus three U-bolts
   g. Three U-bolts (no gasket)
   h. Three steel shipping bands.

3. Condulet with a special 11-gauge steel cover installed tightly using the two screws provided by the manufacturer--under the following conditions:

   a. No gasket
   b. Tecknit-Elastomet gasket
   c. Tecknit #721101 compound gasket
   d. Mating surfaces brushed and polished prior to assembly plus Tecknit #721101 compound gasket and three U-bolts
   e. Cover welded to condulet.

4. Condulet with special 11-gauge steel cover that has been flame-sprayed with tin, prior to being tightly installed using the two screws provided by the manufacturer--under the following conditions:

   a. No gasket
   b. Three U-bolts (no gasket)
   c. Mating surfaces brushed and polished prior to assembly
   d. Mating surfaces brushed and polished prior to assembly plus three U-bolts
   e. Mating surfaces brushed and polished prior to assembly plus three steel shipping bands
   f. Mating surfaces brushed and polished prior to assembly plus Chomerics 4331 gasket
   g. Tecknit #721101 compound gasket
   h. Tecknit #721101 compound gasket plus three U-bolts

5. Condulet with special 11-gauge steel cover that has been flame-sprayed with zinc, prior to being tightly installed using the two screws provided by the manufacturer--under the following conditions:

   a. No gasket
   b. Three U-bolts
   c. Mating surfaces brushed and polished prior to assembly
   d. Mating surfaces brushed and polished prior to assembly plus three U-bolts
   e. Tecknit #721101 compound gasket.

Figure 34. Summary of combination of condulets, gaskets, and covers tested.

gasket was formed to achieve a uniform thickness of at least 1/2 in. of steel wool prior to compression by tightening the cover plate.

The Tecknit* gaskets were supplied by the manufacturer especially for use on Type C condulets. These were approximately 1/16 in. thick.

Conductive-compound gaskets were formed from Chomerics 4331 and Tecknit 721101 conductive compound by applying a liberal bead of the compound around the entire periphery of the condulet/cover mating surface prior to installing the cover. The compound was not allowed to "setup" or cure prior to assembly or testing.

Three methods of securing the condulet covers to the condulets were tested. One was the standard method of using the two screws supplied by the manufacturer at either end of the cover. The second method included the addition of three U-bolts evenly spaced across the cover (Figure 35) to insure uniform pressure across the condulet lid. The third method used three tightly fastened (with a banding machine)** metal-shipping bands† (Figure 36) in place of the U-bolts.

Heated Couplings. A number of samples were tested to determine the effects of heating on the EMP-shielding effectiveness of a conduit coupling joint (such as caused by welding near the joint). The samples were made up of 5-ft sections of rigid-steel conduit joined by a taper-threaded coupling giving an overall length of approximately 10 ft. This assembly was then used as the ground leg of the transmission line. The assemblies prepared and tested were:

a. Four samples of a conduit with rusted threads that were brush-coated with Chomerics 4331 conductive compound (normal viscosity) prior to assembly.

b. One sample of a conduit with factory-galvanized threads that was brush-coated with Chomerics 4331 conductive compound (normal viscosity) prior to assembly.

c. One sample of a conduit with factory-galvanized threads that was coated with Eccoshield VX conductive compound†† prior to assembly.

---

* Tecknit Elastomet, EMI/RFI shielding, environmental sealing material, using convoluted wire encased in silicone, distributed by Technical Wire Products.

** Signode Tensioner, Model P 3/8, size 3/4, distributed by Signode Corp., Chicago, IL.

† Signode steel banding stock, 0.015 in. x 1/2 in., distributed by Signode Corp.

†† Manufactured by Emerson and Cuming, Inc., Canton, MA.

Figure 35. Type 35C condulet with 11-gauge steel cover and three U-bolts.

Figure 36. Type 35C condulet with 11-gauge steel cover and steel shipping bands.

All samples were wrench-tightened to 200 ft-lb of torque prior to testing. The sense wire passing through the conduit was asbestos-insulated to prevent deterioration of the insulation under application of heat.

Each joint was heated with an oxygen/acetylene welding torch with the flame adjusted to the level normally used for brazing steel 1/8 to 1/4 in. thick. The torch was held so that the maximum heat portion of the flame was applied directly to the conduit and it was moved in such a way that the heat was applied evenly around the entire circumference of the conduit at the specified lateral distance from the coupling. The heat was applied for 60 sec in each test during which the conduit became red hot. Figure 37 shows a test conduit after several applications of heat.

Reference data were taken for the assembled conduit prior to heating. The test setup was not again altered except for application of heat at the test locations.

Figure 37. Heated coupling sample shown after having been heated.

The galvanized-thread sample with Chomerics 4331 conductive compound was heated at the coupling three times for 60 sec each--each period being a simulation of a stick weld around the entire circumference of the conduit. Test data were taken after each heating period to determine the effects of repeated heat application on the EMP-shielding effectiveness of the joint.

Rusted Conduit - Field Rust vs Laboratory Rust. To compare the EMP shielding of field-rusted and laboratory-rusted conduits, samples of 2-in. conduits and couplings were obtained from the North Dakota SAFEGUARD site. The samples had rusted because they had been left outside at the site, with soil and weather contributing to the corrosion. Only six

conduit sections (sufficient for three test samples) were available; therefore, a test sample could not be spared to measure the thickness of the field rust. However, it was visually determined that the rust had a very uniform appearance and sufficient depth so that pitting and loss of shape of the threads were just beginning to occur. In general, visual inspection indicated a rust depth comparable to the laboratory-rusted samples reported in Chapter 4.

The 2-in. conduit samples received were 4 ft long with a factory-galvanized thread on one end and the rusted field-cut thread on the other end. The couplings received were plastic (vinyl) covered and intended for use with the vinyl-coated conduit used at the site. In the preparation of samples at CERL, the vinyl sleeves were cut away from the couplings at each edge in order to simplify sample assembly. Samples were assembled for testing in a parallel conduit transmission line (using 1-in. conduit). The completed test sample included two of the 4-ft long field-rusted samples with the rusted field-cut threads mated with the field-rusted coupling. The factory-galvanized ends of the conduit samples were thoroughly cleaned and mated with a female 2 in. to 1 in. reducer. One-in. conduits, 1 ft in length, were then threaded onto each reducer, thus making up a test sample about 10 ft long that was installed in the 1-in. conduit-test setup (Figure 38).

Figure 38. Rusted 2-in. conduit sample as installed in parallel conduit transmission line (showing reducer).

For comparison purposes, 2-in. conduit samples with laboratory-rusted threads were prepared and tested. The samples were identical to the field-rusted samples described above, except that in the specially designed environmental corrosion chamber described in Chapter 4, the threads were rusted by subjecting them to high relative humidity (near 100 percent) and a temperature of about 150°F for 2 wk. Couplings used with the laboratory-rusted samples were field-rusted and from the same lot as used with the field-rusted samples.

Data were taken with the joints tightened to various tightness levels, ranging from a minimum of hand-tight (approximately 10 ft-lb of torque) to a maximum of 400 ft-lb of torque.

Rusted Conduit Repeatability. To investigate the repeatability of the data obtained from tests of conduit with rusted threads, 10 samples were prepared using laboratory-rusted 1-in. rigid-steel conduit sections, each 5-ft long, coupled with nonrusted tapered couplings. In all 10 cases, no effort was made to clean the threads and no conductive compound was applied to the threads prior to assembly. Data were taken with each sample hand-tight (approximately 10 ft-lb of torque) and again when the joints were wrench-tight (approximately 200 ft-lb of torque).

Lock Nuts. Lock nuts (Figure 39) were tested by using two nuts to join a 5-ft section of 1-in. rigid-steel conduit to a 2-in. end cap that had a hole drilled in it to accept the conduit. The end cap was installed on a 6-in. section of 2-in. conduit that was joined with a reducer to another 5-ft section of 1-in. rigid-steel conduit (Figure 40). This whole assembly was then installed as the ground leg of a parallel conduit transmission line. All joints, with the exception of the lock-nut joint, were sufficiently tightened (after having been coated with Chomerics 4331 conductive compound) to assure that the signal that was induced in the sense wire passing through the assembly was the result of the lock-nut joint.

Data were taken with the lock nuts both hand-tight (approximately 10 ft-lb of torque) and wrench-tight (approximately 200 ft-lb of torque), with the nuts installed in their normal orientation* and backwards from their normal orientation. Data were also taken with and without a conductive compound having been applied to the lock nuts and the mating surfaces prior to assembly.

Threaded Hubs. In this test, the 1-in. threaded hubs (Figure 41) were used instead of lock nuts to join the 1-in. conduit to the 2-in. end cap described above. Figure 42 shows the resulting assembly. All joints other than the threaded hub were coated with Chomerics 4331 conductive compound and then assembled sufficiently tight to assure

---

* Installed so that the edges of the lock-nut bit into the surface of the end cap when tightened.

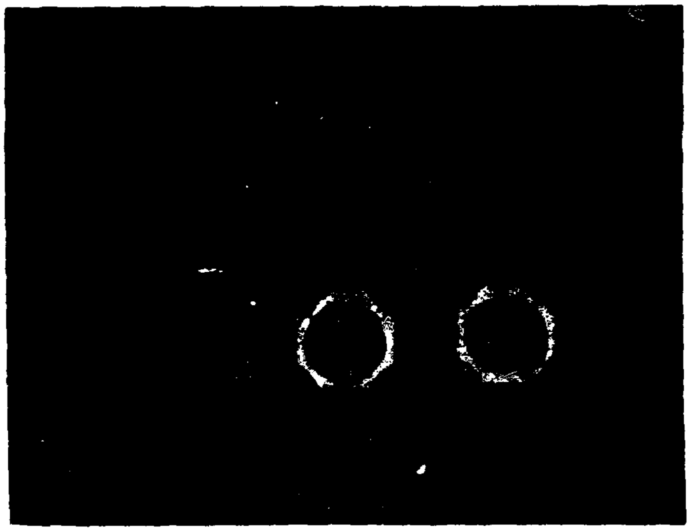

Figure 39. Lock-nut tests samples.

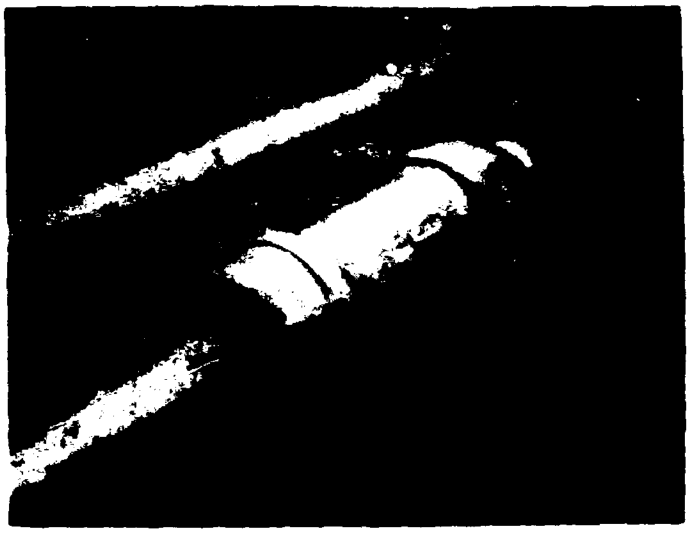

Figure 40. Close-up of lock-nut test assembly.

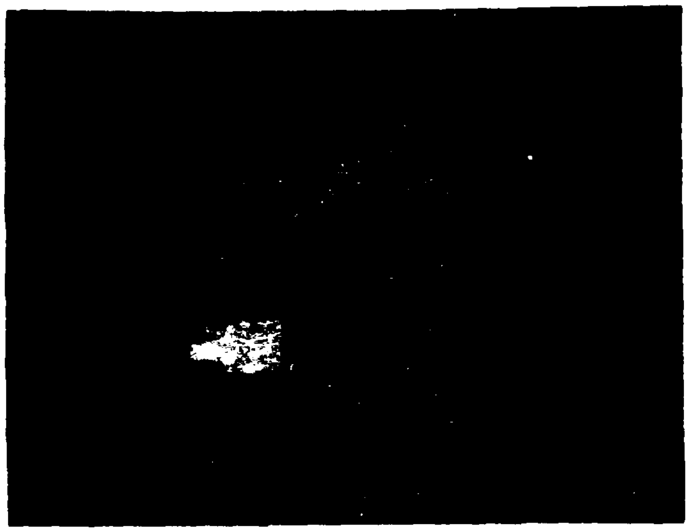

Figure 41. Exploded view of threaded-hub test sample.

Figure 42. Close-up threaded-hub test assembly.

that any signal induced in the sense wire was attributable to the hub joint being tested.

The hubs were tested using the rubber ring provided by the manufacturer. Conductive compound was applied to the threads of some of the hubs prior to assembly. Initially, each hub was tightened to 5 ft-lb of torque, and then subsequently tightened in increments up to 100 ft-lb of torque or to the tightness where the magnitude of the signal induced in the sense wire was too small to measure.

Transverse-Slotted Conduit. These tests were conducted using a conduit section that had been modified to produce a relatively large EMP leakage. This was done to determine the relationship between the I_{SC} wave form and the location of the sense wire with respect to the EMP-leakage location.

A 10-ft section of rigid-steel conduit was modified by cutting a transverse slot at its center. The slot was approximately 0.045 in. wide, and was cut approximately one-half way through the conduit. This conduit was then used as the ground side of the transmission line, and a single sense wire was installed inside it. As in all of the previous tests, one end of the sense wire was connected to the conical end cap and the other was grounded to the inside of the shielded enclosure. Care was taken to properly install the test conduit in the transmission line so that variations in the I_{SC} wave form could be related to the orientation of the slot and the relative location of the sense wire.

Tests were conducted with the test conduit in each of three orientations shown in Figure 43, and with the sense wire adjacent to the slot, in the center of the conduit (midway between slot and solid wall) or adjacent to the solid wall opposite the slot.

Differential Mode Sense Wire. All previous tests used a common-mode sense wire, where one end of the #12 copper wire was grounded to the injection end of the test sample. As discussed in Chapter 4, this common-mode arrangement provides a worse-case condition for signal pickup within conduit runs. However, it does not indicate actual signal magnitudes induced by EMP on differential-pair circuits that are not grounded to the conduit system. Differential-mode, sense-wire tests were performed to investigate the levels of signals induced under such conditions that are representative of actual field conditions. These measurements were taken in much the same manner as the common-mode measurements, except that a two-conductor sense wire was used--neither conductor of which was connected to the conduit system, either at the injection end or in the shielded enclosure. The signals measured on the differential-sense wire are smaller in magnitude than the signals obtained from a common-mode sense wire for equivalent test samples; therefore, all differential-mode sense wire tests were performed on samples exhibiting high EMP leakage in order that the signals obtained would be within the instrumentation measurement range.

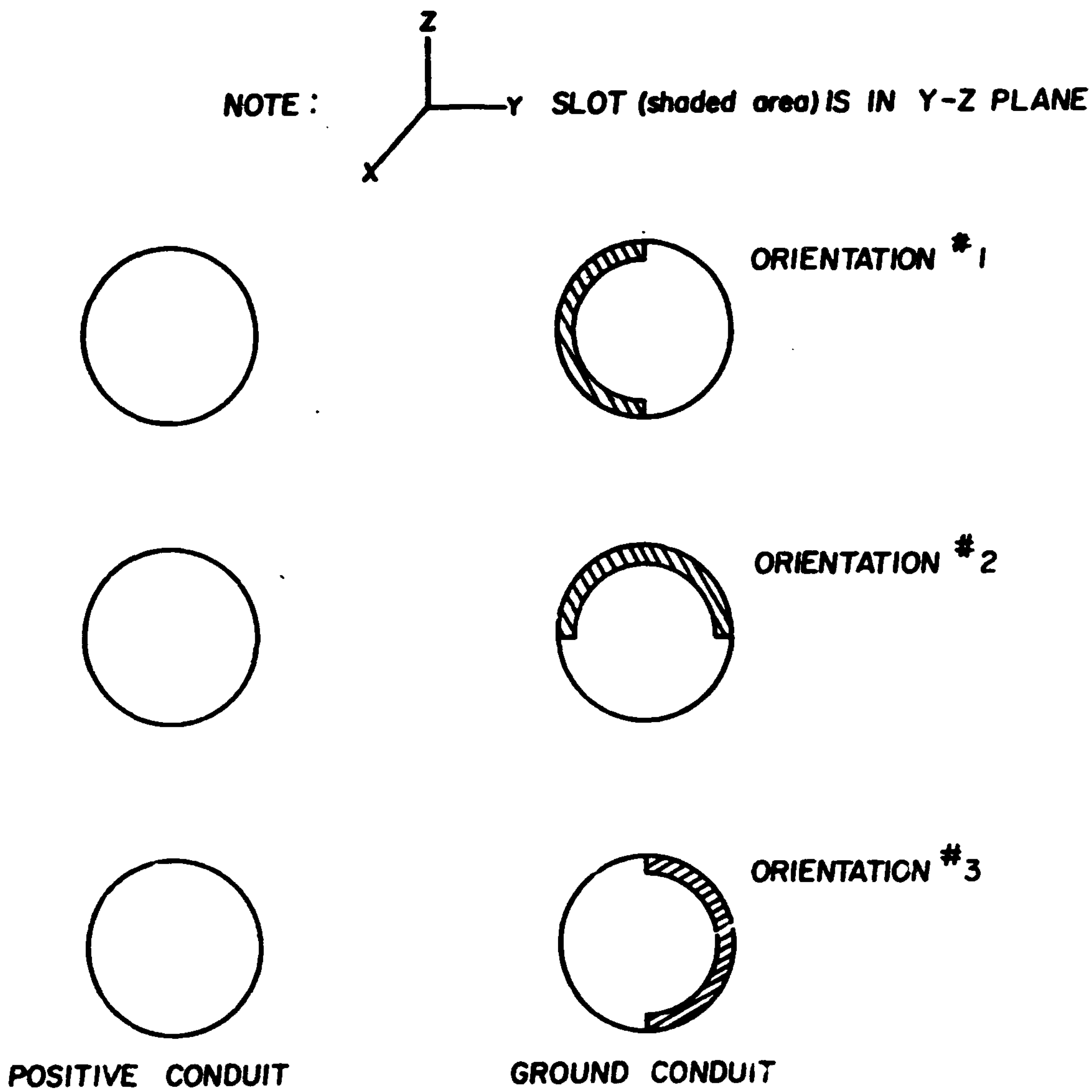

Figure 43. Cut-away end view of transmission line showing orientation of slot for transverse-slotted conduit tests.

Differential sense-wire tests were performed on two test samples. One was a 1-in. conduit 10 ft in length with a transverse slot cut into the sample at its center, as described in the previous section. The slot was cut half through the conduit using a standard hacksaw blade that established a slot width of approximately 0.045 in. The other sample was a 2-in. conduit, 10 ft in length with a coupling at the center. The threads of the coupling and of the conduit ends had been heavily and uniformly field-rusted prior to conduit assembly. All threads at the coupling were wrench-tightened to 400 ft-lb of torque prior to testing. The coupling was not disturbed during these tests.

In each sample described above, five sense-wire configurations were tested. These are described as follows:

a. Twin lead with parallel common-mode ground wire. The twin lead used was a 300-ohm parallel-wire transmission line of the type commonly used for VHF television antenna lead-in wire. The twin-lead pair was shorted together at the pulser end of the test sample. The common-mode grounded sense wire was used in most of the tests described in this report; in addition, in order to maximize coupling between the common-mode wire and the twin lead, it was taped to the twin lead in such a way that one conductor of the twin lead was adjacent and parallel to it.

b. Twin lead only. The twin lead was used by itself, with its conductors shorted together at the pulser end.

c. Twisted pair. The sense wire was a pair of 20-gauge stranded wires that had been twisted together with approximately one twist per inch. The wire used was MIL-W-76B hook-up wire, part number designation MW-C-20(7)-U, manufactured by Belden.

d. Shielded-twisted pair, grounded shield. The sense wire used was RG-108 shielded twisted pair, with the pair of wires shorted together at the pulser end, and the shield grounded at both ends.

e. Shielded-twisted pair, floating shield. The sense wire used was again RG-108, with the pair of wires shorted at the pulser end, and the shield left floating.

Effects of Conduit Length on I_{SC}. These tests were conducted to investigate the effect of conduit length on the resulting I_{SC} wave form for the common-mode configuration. In preparing this test sample, a 1-ft section was cut from the center of sample three of the rusted 1-in. conduits discussed in the section on Rusted-Conduit Repeatability. This sample provided a relatively large I_{SC} signal as originally tested. The 1-ft assembly was threaded on both ends and couplings were wrench-tightened to these threads. Various lengths of conduit (up to 1 in.) could be added to this sample to make a test conduit of any desired length without disturbing the rusted coupling. The assembled sample was inserted into a transmission line setup for testing. Figures 44 and 45

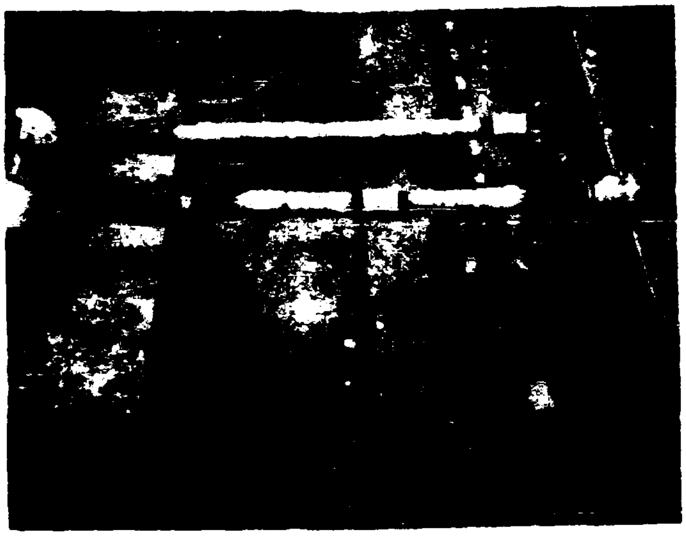

Figure 44. Three-ft long sample as installed.

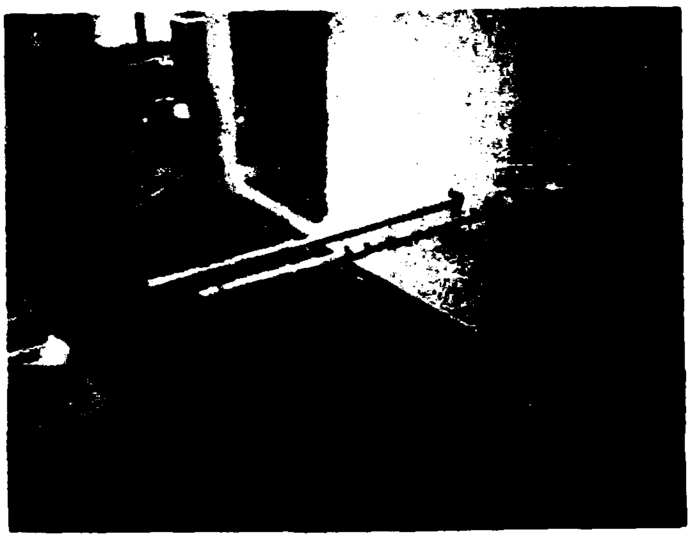

Figure 45. Four-ft long sample as installed.

show the 3-ft and 4-ft test samples. Throughout the tests of the various conduit lengths, extreme care was taken not to apply torque either directly or indirectly to the coupling joint. Thus, any changes in the I_{SC} wave form were due to changes in the conduit length.

Test Results. This section describes the results obtained from testing the samples described in the previous section.

Explosion-Proof Unions. Test results for the 1-in. and 4-in. explosion-proof unions are tabulated in Table 6. No signal was measured with a wrench-tightened 1-in. union or with the standard (ribbed-mating surface) or modified (flat-mating surface) 1-in. unions. The shielding effectiveness of the 4-in. unions was not as good as with the 1-in. unions. This was probably because of the 4-in. union's larger mating-surface area--which provides a greater area over which leakage can occur--and because of its larger diameter. For an equivalent torque, the pressure per unit area on the threads will be considerably less on the larger diameter conduit.

Four-In. Conduit Coupling. Results obtained during the tests of the 4-in. conduit couplings are tabulated in Table 7. The results are similar to those presented in Chapter 4 for 1-in. couplings:

a. A properly assembled coupling joint (clean threads, wrench-tight, with conductive compound on the threads prior to assembly) provided sufficient EMP shielding to reduce the signal on the sense wire to a level equivalent to a solid conduit.

b. The largest leakage signals were observed with coupling joints with rust on the threads or with couplings that had not been sufficiently tightened.

c. The application of conductive compound (Chomerics 4331) to the conduit threads prior to assembly of the coupling joint resulted in a small improvement in shielding effectiveness (as compared to a similar joint assembled without conductive compound).

Flexible Conduit. Test results from the samples of non-RFI tight flexible conduit are listed in Table 8. The tightness of the fittings on the ends of the sections of flexible conduit had no significant effect on shielding effectiveness. Thus, it was apparent that the signal on the sense wire was being induced by leakage through the flexible section itself. This was not a diffusion signal, but rather occurred because the flexible section of the conduit was not a continuous piece of metal; thus, there are many possible leakage points. The use of a ground wire in parallel with the flexible conduit section provided only a small decrease in leakage current. It is obvious from Table 8 that, even under the most ideal conditions, this type of flexible conduit produces a serious degradation in shielding effectiveness.

Table 6

Explosion-Proof Union Test Data

Sample	$I_{short\ circuit}$ Peak (mA)	Rise Time (μsec)
1-In. UNIONS		
UNY, Std, HT	5.1	1.4
UNY, Std, WT (150 ft-lb)	---	---
UNF, Std, HT	19.3	1.1
UNF, Std, WT (150 ft-lb)	---	---
UNF, Mod, HT	21.1	1.0
UNF Mod, HT w/4331	6.2	0.9
UNF, Mod, WT, w/4331 (150 ft-lb)	---	---
4-In. APPLETON UNIONS		
UNF, Std, HT	290.0	NT
UNF, Std, WT (1200 ft-lb)	1.25	3.5

NOTES: w/4331 = Chomerics 4331 conductive compound
HT = Hand-tight
WT = Wrench-tight
--- = Value too small to measure (< 50 μamps
NT = Data not taken
Std = Standard coupling
Mod = Modified (see section on Explosion-Proof Unions)

Table 7

Test Results Using 4-In. Conduit Couplings

No.	Test Sample Description	Torque Ft - lb	Short Circuit Current Peak (mA)	Open Circuit Voltage P-P (mV)	V_{100} Peak (mV)	I_{100} Peak (mA)
31	Non-rusted with Chomerics 4331 compound brush-applied	HT	34	2,000	480	4.6
		400	--	-----	----	---
32	Rusted, without compound	HT	350	21,000	6,000	43
		400	65	1,800	580	4.6
		1000	4.6	NT	NT	NT
33	Rusted with Chomerics 4331 compound brush-applied	HT	276	2,100	1,040	10.8
		400	15.9	160	70	.62
		1000	1.5	NT	NT	NT
34	Rusted with Chomerics 4331 compound, thinned-stick applied	HT	535	11,600	3,600	30.8
		400	92.5	720	NT	NT
		1000	10.8	70	NT	NT

NOTES: --- = Value too small to measure (< 50 μamps).
NT = Data not taken.

Table 8

Interior Non-RFI Tight 1-In. Flexible Conduit Test Data

Sample	Condition	$I_{Short\ Circuit}$ Peak (mA)	Rise Time (μsec)	Fall Time (μsec)
#1 HT	Without ground strap	1725	1.1	4.2
#1 HT	With ground strap	800	.85	3.8
#2 HT	Without ground strap	1410	1.0	4.4
#2 HT	With ground strap	874	0.7	3.3
#2 WT	Without ground strap	2060	0.8	3.6
#2 WT	With ground strap	874	0.8	3.6

Test results from the various types of RFI-tight flexible conduit are listed in Table 9. Figures 46 through 49 show the I_{sc} wave forms that were measured during some of the test conditions.* These wave forms contain both leakage-current (fast-rise time) and diffusion-current (slower rise time) components. In most cases, the diffusion-current component amplitude is larger; however, as shown in Figures 50 and 51, the leakage-current magnitude can be greater. This was a test of the specially designed conduit section that used an automotive screw-type hose clamp to secure one end of the braid. These conduits were significantly better than the non-RFI tight flexible conduits, though not as good as solid conduits.

Condulets, Gaskets, and Covers. Test results conducted on condulets using various covers and gasket materials are shown in Table 10. These data indicate that no combination of cover, securing method, and gasket-material reliability resulted in an I_{sc} of less than 1 mA. More specifically:

a. None of the gasket types tested provided a substantial improvement in shielding effectiveness over the standard cover without a gasket.

b. The Tecknit gasket actually degraded the shielding effectiveness from that measured with the cover only (without a gasket).

c. Conductive compounds provided some (but not a substantial) improvement in shielding effectiveness.

d. The use of U-bolts or bands to secure the condulet cover provided a small improvement in shielding effectiveness when no gasket was used, but reduced the shielding effectiveness when a gasket was used.

The most effective cover was an 11-gauge steel flat cover that had been flame-sprayed with a tin coating and installed without a gasket. Some additional improvement in shielding effectiveness was achieved when conductive compound and U-bolts were also used.

The data also show that when the cover is welded onto the condulet, eliminating the gap between the cover and the condulet, the signal induced by EMP leakage is too small to measure. This substantiates the conclusion that the leakage source was the gap between the cover and the condulet. The maximum shielding effectiveness would therefore be achieved by reducing the gap as much as possible or eliminating it. In addition, the rise time of the I_{sc} pulse, for all conditions tested, was less than 10 μsec, indicating that leakage effects were the primary source of the induced signal.

* Data were taken with the Tektronix P6021 current probe and should be a fairly accurate representation of the current wave form.

Table 9

Test Results Using RFI-Tight Flexible Conduit

Description	I_{sc} Peak (mA)	τ_r (μsec)
1 1/2-in. PVC covered - no braid	280-500mA*	55-60
1 1/2-in. standard steel flexible with double-galvanized steel braid (pt. #2198-700)	25	125
4-in. standard steel flexible with galvanized steel braid	5.9	280-310
4-in. standard steel flexible with 1-in. wide copper braid in parallel	5	-
4-in. standard steel flexible with 2 1/2-in. wide copper braid in parallel	4.4-4.7	-
1 1/2-in. Hypermaflex with stainless-steel braid	Leakage 2.6 Diffusion 70	4 175
1 1/2-in. Hypermaflex with stainless-steel braid	94	150
1 1/2-in. Hypermaflex with stainless-steel braid removed	185	80
1 1/2-in. Hypermaflex with two layers of galvanized steel braid (part# 306971)	Leakage 1.7 Diffusion 10.8-12	8 800-1000
1 1/12-in. special design using hose clamp on one end	Leakage 40 Diffusion 16	120 Indeterminate

NOTE: Where more than one value is given for any test condition, multiple samples were tested.

* These data differ from earlier data reported under separate cover (preliminary reports), because the earlier data were taken with a current probe with a low-frequency response, which was insufficient to accurately detect the I_{sc} wave form.

Figure 46. I_{sc} wave form--1 1/2-in. flexible PVC-covered conduit (i = 50 mA/div; t = 50 μsec/div).

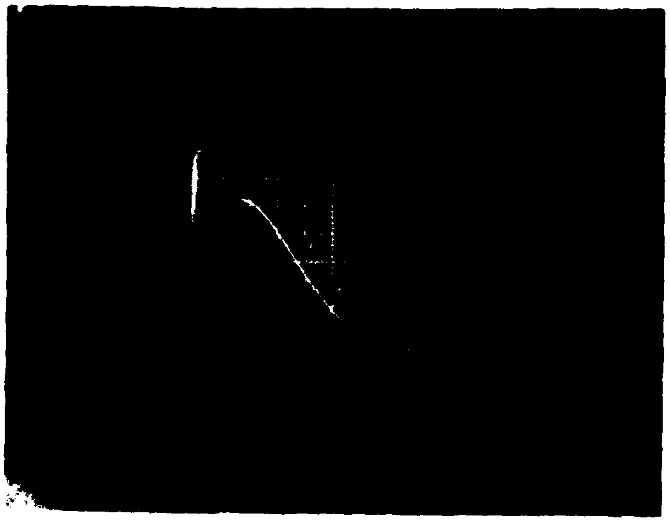

Figure 47. I_{sc} wave form--4-in. standard steel flexible bellows with galvanized steel braid (i = 1 mA/div; t = 50 μsec/div).

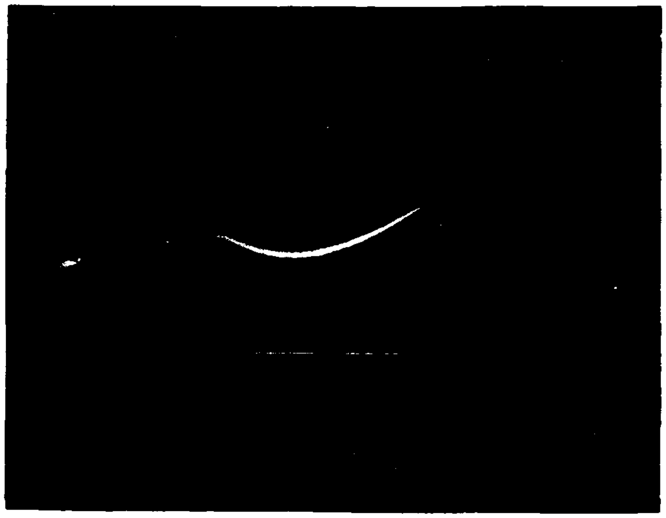

Figure 48. I_{sc} wave form--1 1/2-in. Hypermaflex bellows with double-galvanized steel braid (i = 40 mA/div; t = 10 μsec/div).

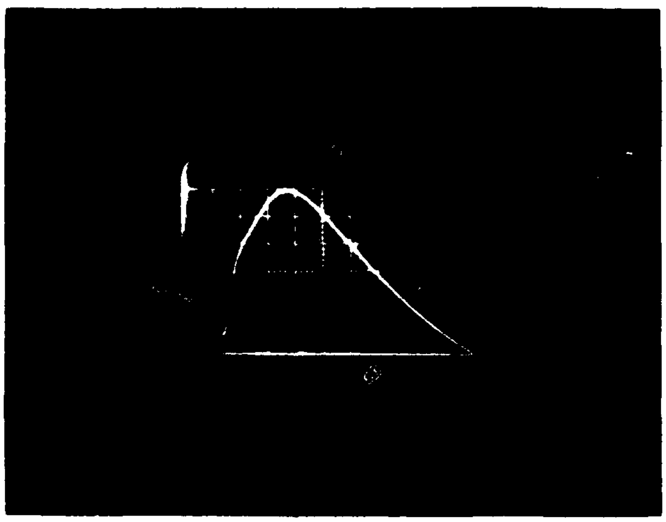

Figure 49. I_{sc} wave form--1 1/2-in. Hypermaflex bellows with double-galvanized steel braid (i = 2 mA/div; t = 0.5 msec/div).

Figure 50. I_{sc} wave form--1 1/2-in. special design flexible conduit (i = 10 mA/div; t = 50 μsec/div).

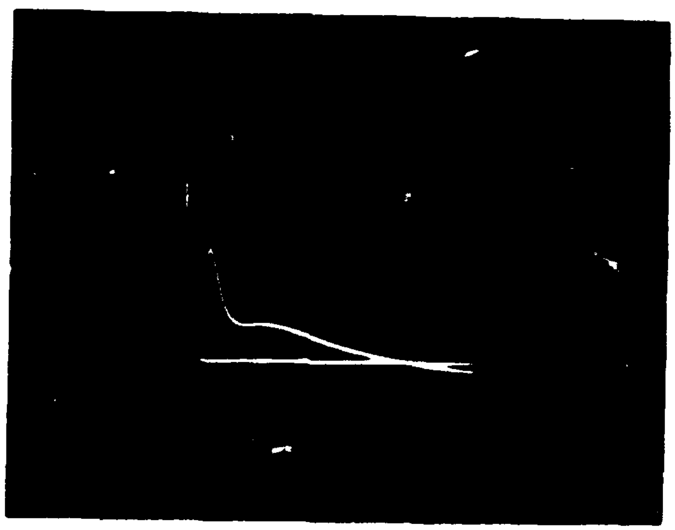

Figure 51. I_{sc} wave form--1 1/?-in. special design flexible conduit (i = 10 mA/div; t = 0.5 msec/div).

Table 10

Results of Tests on Condulets, Covers, and Gaskets

Condition	I_{sc} peak (mA)
1. No cover	133-161
2. Stamped 16-gauge steel (K100) cover (screws always tightened)	
a. No gasket	23
b. Steel-wool gasket	5-5.7
c. Chomerics 4331 gasket	1.3-3.4
d. Tecknit-Elastomet gasket	30
e. Tecknit-Elastomet gasket + three bands	48
f. Tecknit-Elastomet gasket + three U-bolts	31.5
g. Three U-bolts (no gasket)	9.2-11.6
h. Three bands (no gasket)	8.6
3. 11-gauge steel cover (screws always tightened	
a. No gasket	31.5
b. Tecknit-Elastomet gasket	34
c. Tecknit #721101 compound gasket	30
d. Surface brushed and polished + Tecknit #721101 compound gasket + three bolts	18
e. Cover welded to condulet	too small to measure
4. 11-gauge steel cover flame-sprayed with tin (screws always tightened)	
a. No gasket	5.3-6
b. Three U-bolts (no gasket)	.32-4.9
c. Surface-brushed and polished	2-4.4
d. Surface-brushed and polished + three bolts	1.4-3.6
e. Surface-brushed and polished + three bands	4.2-5.5
f. Surface-brushed and polished + Chomerics 4331 gasket	1.2
g. Tecknit #721101 compound gasket	3.4
h. Tecknit #721101 compound gasket + three U-bolts	2.9
5. 11-gauge steel cover flame-sprayed with zinc (screws always tightened)	
a. No gasket	2.8-12.8
b. Three U-bolts	11-20
c. Surface-brushed and polished	2.2-5.8
d. Surface-brushed and polished + three U-bolts	0.24-2.05
e. Tecknit #721101 compound gasket	30

Heated Couplings. Table 11 lists the results obtained from the heated coupling tests. These data indicate that:

a. Welding distances of 3 in. or greater from a coupling will not change the shielding effectiveness of the conduit assembly.

b. Heating at the coupling (equivalent to welding) improves the shielding effectiveness of pre-rusted conduit and does not change the shielding effectiveness of conduit assembled with clean factory-galvanized threads and conductive compound.

The results also indicate that repeated application of heat will not degrade conduit-shielding effectiveness.

Rusted 2-In. Conduit--Field Rust vs Laboratory Rust. Table 12 lists the results of the tests conducted on the rusted 2-in. conduit. When tested under similar conditions, there is no apparent difference in shielding effectiveness between the laboratory-rusted and field-rusted samples. For purposes of this report, laboratory-rusted samples will give adequate indication of the performance of rusted samples.

Rusted 1-In. Conduit Repeatability. Data obtained during the tests of the 10 rusted 1-in. conduit samples are listed in Table 13. These data indicate that, under identical test conditions, the measured peak value of I_{sc} for these rusted conduit samples (which were nearly identical) varied from a maximum 34 mA to a minimum of no signal detected (<50 μamp). Thus, the repeatability of the test results for rusted conduit samples is not very high. This is probably the result of the unevenness of the rust and the uncertainty of the metal-to-metal contact that can be obtained when the rust is present. It also probably indicates that in some cases the rust can be knocked off in tightening the coupling. A worse case leakage signal of 10-50 mA is probably a safe assumption for properly tightened rusted conduit.

Lock Nuts and Threaded Hubs. Results of the shielding-effectiveness tests on the threaded hubs are shown in Table 14. Results of shielding effectiveness on the lock nuts are shown in Table 15. When sufficiently tightened, both hubs and lock nuts can provide very effective EMP shielding, especially if the joint is coated with conductive compound prior to assembly.

Transverse-Slotted Conduit. Results of this investigation are summarized in Table 16. It can be noted from this summary that the diffusion-current component (I_d) was relatively constant throughout the test. However, this is not the case with the leakage-current component (I_L). The location of the sense wire within the conduit had a considerable effect on the leakage component of the I_{sc} wave form. Earlier studies had shown that this was not true for leaking couplings in which the leakage source was uniform around the periphery; thus the location of the sense wire is only important if the leakage is not uniform around the circumference of the conduit.

Table 11

Heated Coupling Test Data

Sample and Condition	$I_{\text{Short Circuit}}$ (mA) for Various Heat Application Distances from Coupling					
	Ref.*	12 in.	6 in.	3 in.	0 in.	After** Cooling
Pre-rusted, sample #1	2.6	2.6	2.7	NT	--	.007
Sample #2	.17	.175	.182	NT	--	NT
Chomerics 4331 #3	.131	NT	.139	.139	--	NT
Compound wrench-tight sample #4	0.025	NT	--	NT	--	0.015
Clean galvanized threa. 4331	--	NT	--	NT	--	NT
Clean galvanized thread EC VX	--	NT	--	NT	--	NT

NOTE: In all cases, τ_r^1 = 3 - 4μsec.

$^1\tau_r$ = rise time (0 - 90 percent of peak).

NT = Data not taken.

-- = Value too small to measure.

*Reference data taken prior to application of heat.

**Conduit and coupling were allowed to cool and ·ge for 24 hr after heating.

Table 12

Results of Tests Using Rusted 2-In. Conduit--Field Rust vs Laboratory Rust

	Hand Tight		50		100		200 (WT)		400	
	I_{sc}	V_{oc}	I_{sc}	V_{oc}	I_{sc}	V_{oc}	I_{sc}	V_{oc}	I_{sc}	V_{oc}
Lab rust - No Compound τ_r 2.9-4.2μsec	* 33A	490V 170V	- -	- -	- -	- -	0.76A 0.66A	5.8V 9V	- -	- -
Lab rust - Compound τ_r 1.6-3.8μsec	2.6A 1.75A	19.5V 39V	2.4A 2.1A	9.4V 7.2V	1.75A 0.6A	9.6V 10.8V	0.88A 225mA	5.5V 2.85V	116mA 180mA	1.02V 0.66V
Field rust - No Compound τ_r 1.6-3.6μsec	1.8A	335V	1.75A	50V	1.0A	19.5V	0.37A	9.4V	290mA	4.5V
Field rust - Compound τ_r 0.8-5.2μsec	0.9A 34A	12V 77.5V	2.05A 0.52A	35V -	0.45A 0.35A	17.5V 4.9V	200mA 225mA	8.2V 2.5V	76-82mA 57mA	1.12-1.14V 1.75V
No rust on conduit - No Compound (with field rusted coupling) τ_r 1.9-4μsec	0.43A	5.0V	94	0.92V	17.5mA	0.48V	25mA	0.15V	3.4mA	-

Table 13

Results of Repeatability Tests Using Rusted 1-In. Conduit

Sample	Hand Tight			Wrench Tight		
	I_{sc} (mA)	τ_r (μ)	V_{oc} (V)	I_{sc} (mA)	τ_r (μ)	V_{oc} (V)
1	-	-	-	10	3.8	-
2	360	2	5	22	1.8	-
3	240	1.1	4.6	34	1.4	-
4	560	2.8	2.5	13	3.2	0.125
5	320	3.6	1.5	1.6	8	-
6	920	3.5	0.3	0.1	-	-
7	400	1.82	0.32	0.1	-	-
8	620	3	0.25	3	-	-
9	52	0.62	0.2	none measurable	N/A	N/A
10	200	3.5	0.16	3	-	-

NOTE: Each test sample consisted of two 5-ft sections of 1-in. rigid conduit with laboratory-rusted threads that were joined together using a taper-tapped coupling. No conductive compound was applied to the threads prior to assembly.

Table 14

Results of Shielding-Effectiveness Tests of 1-In. Threaded Hubs

Test Condition		I_{sc} (mA)	τ_r (μsec)
No compound	5 ft-lb	41	0.6
	20 ft-lb	1.72	5.6
	40 ft-lb	0.52	12.4
	60 ft-lb	0.35	-
	80 ft-lb	0.25	-
	100 ft-lb	0.15	-
With conductive compound	5 ft-lb	4.4	3.5
	6 ft-lb	0.24	-
	10 ft-lb	1.3	2.6
	20 ft-lb	0.54	7
	40 ft-lb	No detectable signal (< 50 μamp)	

Table 15

Results of Shielding-Effectiveness Tests of 1-In. Lock Nuts

Test Condition	I_{sc} (mA)	τ_r (μsec)
No compound--normal use*--hand-tight	33	2.3
Wrench-tight	2.4	2.35
Reverse**--hand-tight	108	1.5
Wrench-tight	0.6	6
With compound--normal use*--hand-tight	34	1.88
Wrench-tight	1.1	2.8
Reverse**--hand-tight	96	1.3
Wrench-tight	1.56	1.6

* Normal use--installed so that the edges of the lock nut bite into the surface of the end cap when tightened.

** Reverse use--installed so that the flat side of the nut contacts the surface of the end cap when tightened.

Table 16

Results of Tests Using Transverse-Slotted Conduit

	Location of Sense Wire								
	by slot			at center			by solid wall		
Conduit Orientation*	1	2	3	1	2	3	1	2	3
Function									
peak I_d (mA)	9.3	9.4	9.0	9.2	8.6	9.4	9.6	8.75	9.0
peak I_L (mA)	105	96	118	51.5	64	35	16	17	12.5
peak $I_{overshoot}$ (mA)**	1.6	1.3	1.65	1	0.8	0.7	0.5	-	0.5
peak-peak I_{ring} (mA)	14	8	8	7.5	8	-	1.5	1.5	-
time of overshoot (msec)	0.59	0.52	0.6	0.49	0.5	0.44	0.39	-	0.39
†τ_d (msec)	1.2	1.2	1.2	1.2	1.2	1.1	1.2	1.25	1.2

* Orientation number refers to orientations shown in Figure 43.

** $I_{overshoot}$ refers to I_L overshoot.

† τ_d is the rise time (0 - 90 percent of peak) of I_d.

Differential-Sense Wire. Results of this investigation are summarized in Table 17. As shown in the table, differential-sense wires that are not electrically coupled to other wires have a very small signal induced by an EMP source, which will induce a relatively large common mode I_{SC}. However, the magnitude of the signal induced on the differential-mode sense wire increased significantly when it was closely coupled to a common-mode sense wire on which a large signal was induced.

Variation Conduit Lengths. Figures 52 through 55 show the I_{SC} wave forms that resulted using 1-ft and 11-ft conduit sections. These wave forms are typical of those observed throughout the tests using the various conduit lengths. A summary of the test results is given in Table 18. As shown in the table, the I_{SC} components due to leakage current (I_L) decreased as the conduit length increased. However, the I_{SC} component due to diffusion current (I_d) increased as the conduit length increased, as is expected from the results of Chapter 3.

Conclusions. This study consisted of the measurement of signal pickup resulting from the various conduit test conditions. These data are useful for comparative purposes; however, it is not directly translatable to actual signal levels to be expected on installed wiring. Additional information, which was not available to CERL, is necessary for an analysis to determine the acceptability of the test item for the SAFEGUARD installation. This information includes conduit lengths, types of wires, and the susceptibility of attached circuits.

Some general conclusions that can be drawn from the results presented in this chapter include:

a. Couplings, small unions, and threaded hubs, if properly assembled and tightened, seem to provide no degradation in shielding performance.

b. With proper selection and assembly, most conduit hardware, such as large unions, good flexible conduits, condulets, and lock nuts, will provide some degradation in shielding performance. The degradation is approximately the same in each case ($\approx$1 mA of leakage current for the sense-wire circuit and conduit used in these tests).

c. The heating of couplings had little or no effect on their shielding characteristics.

d. The sense-wire circuit, the presence of other wires inside the conduit, and the length of the conduit run are all factors that affect the signals found on the sense wire when leakage conditions exist.

Table 17

Results of Tests Using Differential-Mode Sense Wire

Sense-Wire Configuration	Max I_{sc} Slotted Conduit	Coupled Conduit
Twin-lead and single-sense wire	30 mA	32 mA
Twin lead alone	0.02 mA	--*
Twisted pair	5 mA	1.6mA
Shielded-twisted pair with grounded shield	4 mA	1.2mA**
Shielded-twisted pair with floating shield	2 mA	0.6mA
Common mode only	not taken	520 mA

*Value too small to measure.
**This configuration had an almost equally large overshoot, making the peak-to-peak reading approximately 2.3mA.

I_L peak

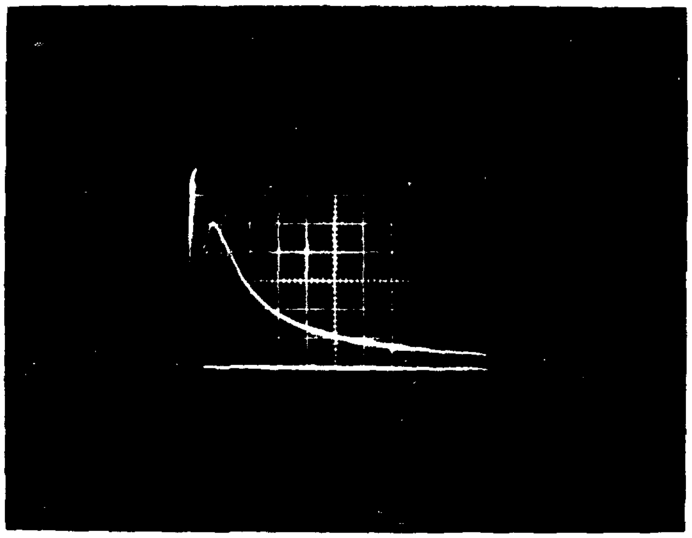

Figure 52. I_{sc} wave form--1-ft conduit length (i = 20 mA/div; t = 10 μsec/div).

I_d peak

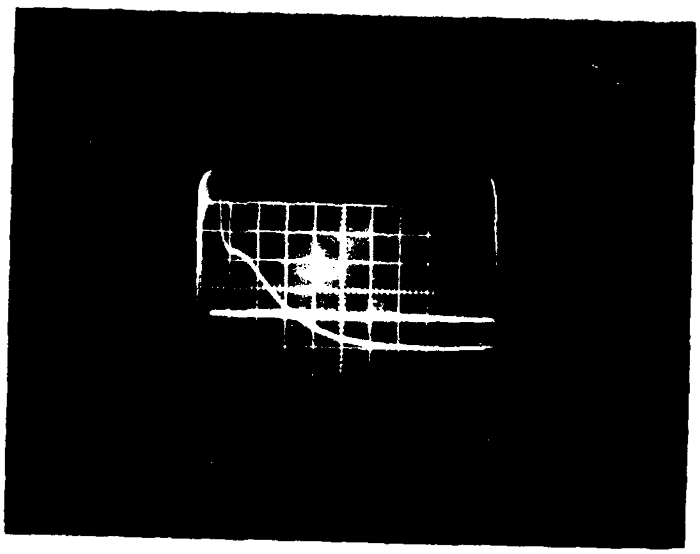

Figure 53. I_{sc} wave form--1-ft conduit length (i = 1 mA/div; t = 1 msec/div).

I_L peak

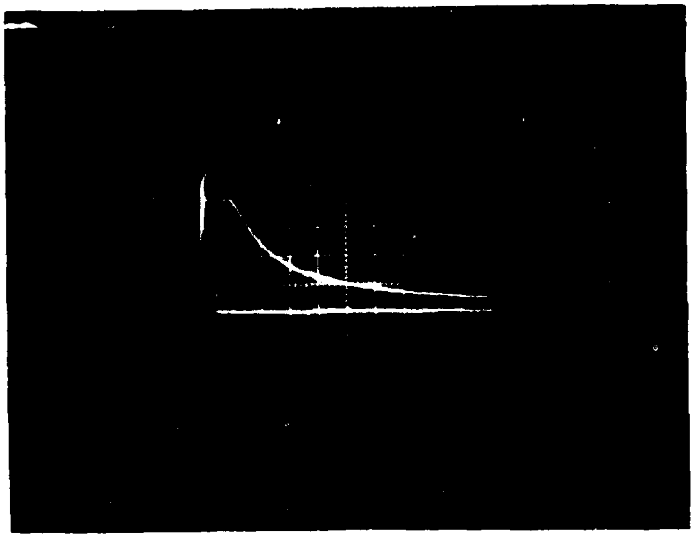

Figure 54. I_{sc} wave form--11-ft conduit length (i = 20 mA/div; t = 10 μsec/div).

I_s peak

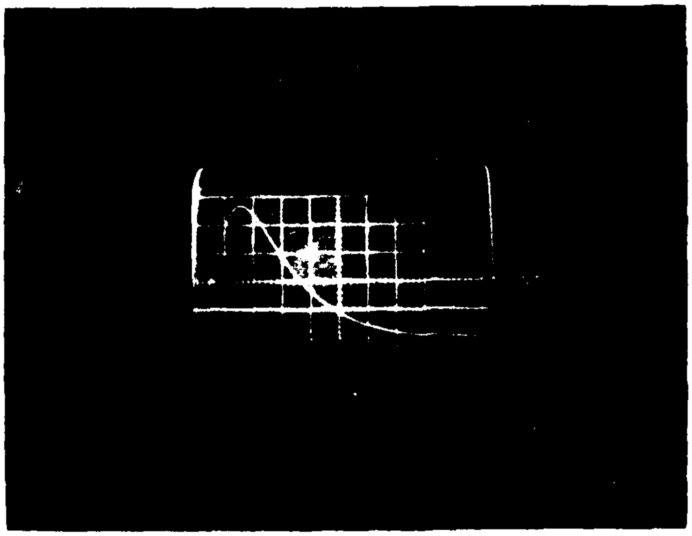

Figure 55. I_{sc} wave form--11-ft conduit length (i = 2 mA/div; t = 1 msec/div).